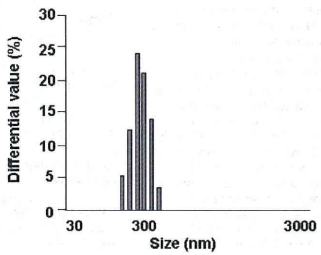

Figure S1. Particle size distribution of CuO-NPs (25 μg/mL) in culture medium assessed by using a laser diffraction particle size analyzer.

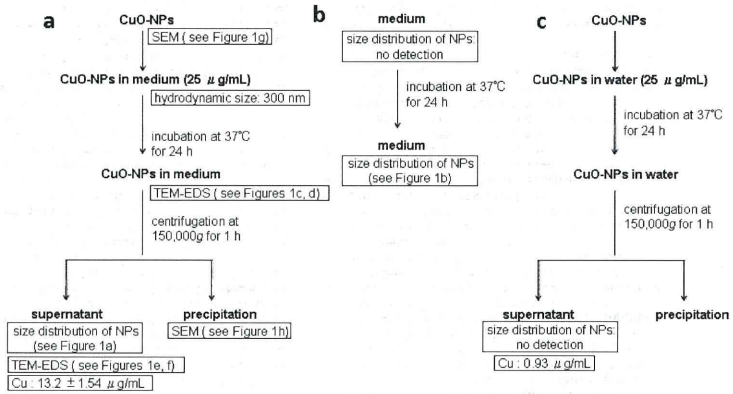

Figure S2. Preparation and characterization of medium containing Cu ions released from CuO-NPs. **(a)** The culture medium with CuO-NPs (25 μg/mL) was incubated at 37□ for 24 h, and then centrifuged. The supernatant was used to estimate contribution of Cu ions released from CuO-NPs into medium to CuO-NPs toxicity. **(b)** Culture medium without CuO-NPs was incubated at 37□ for 24 h, and then particle size distribution was measured with a laser diffraction size analyzer. **(c)** CuO-NPs in water were incubated at 37□ for 24 h, and then centrifuged. No particles were detected in the supernatant.

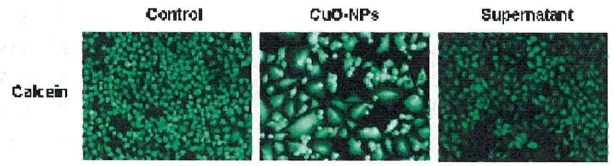

Figure S3. Cell viability as indicated by staining of cells that were exposed to CuO-NPs and the supernatant for 24 h with calcein acetoxymethyl ester (calcein-AM). A549 human lung epithelial cells were cultured in media containing 25 μg/mL CuO-NPs or the supernatant at 37□ for 24 h, and then the number of viable cells was compared to that of the control.

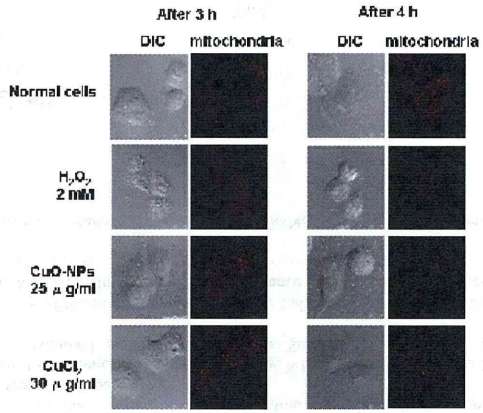

Figure S4. Damage to mitochondria by CuO-NPs. Mitochondrial damage in A549 human lung epithelial cells after exposure to H2O2 (2 mM), CuO-NPs (25 μg/mL), and CuCl2 (30 μg/mL) was measured by using 5,5′,6,6′-tetrachloro-1,1′,3,3′- tetraethylbenzimidazolylcarbocyanine iodide (JC-1; Invitrogen). The accumulation of JC-1 in mitochondria was measured by excitation at 543 nm and detection of fluorescence at 573–607 nm. Damaged mitochondria accumulated less JC-1, and therefore, exhibited less fluorescence. The mitochondria of cells that were exposed to CuO-NPs were damaged after 4 h. Cells that were exposed to CuCl2 also were damaged after 4 h; however, the damage was not as severe as that from CuO-NPs.

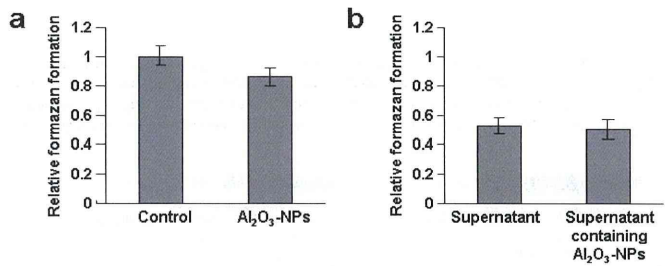

Figure S5. Effect of non-toxic dummy Al2O3-NPs on supernatant toxicity. (a) Cytotoxicity of Al2O3-NPs. The primary size of Al2O3-NPs was 50 nm and the hydrodynamic size was around 160 nm. A549 cells cultured for 48 h were exposed to Al2O3-NPs at a concentration of 25 μg/ml. After 24 h, a WST assay was performed. (b) Effect of Al2O3-NPs on the supernatant toxicity. A549 cells cultured for 48 h were exposed to supernatant and supernatant with Al2O3-NPs. The supernatant contained Cu ions released from CuO-NPs. After 24 h, a WST assay was performed. Zeta potential of Al2O3-NPs was -20.37 mV. Physicochemical character of Al2O3-NPs was previously reported (Xu et al., *Biomaterials* **2010**, 31, 8022-8031).

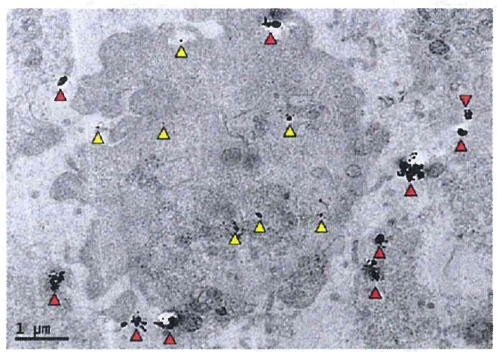

Figure S6. Internalized CuO-NPs observed by TEM. Yellow arrowheads indicate single or smaller (<100 nm) aggregated NPs. Red arrowheads indicate larger (> 100 nm) aggregated NPs. Cells were cultured in medium with 25 μ g/mL CuO-NPs for 24 h, and then living cells were harvested.

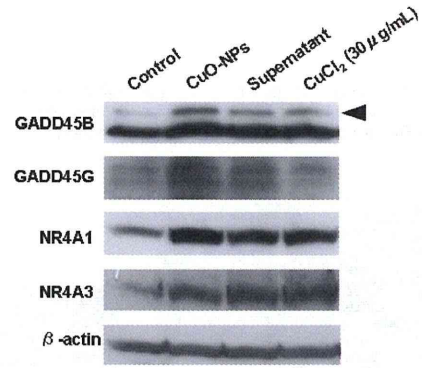

Figure S7. Western blotting analysis to confirm the change of gene expression. A549 cells were cultured for 48 h, and then exposed to 25 μg/mL CuO-NPs, supernatant and 30 μg/mL CuCl 2 for 24 h.

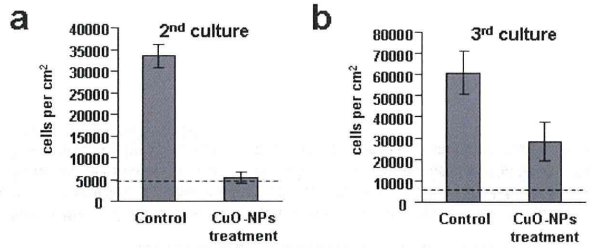

Figure S8. Cell cycle arrest due to CuO-NPs. Cells that were exposed to 25 μg/mL CuO-NPs were isolated, and then seeded in fresh culture medium that did not contain CuO-NPs at a density of 5000 cells/cm2. The left graph shows the number of cells after 72 h. The dotted line shows the number of cells at the time of the seeding. Cell proliferation was not observed. However, when the cells were harvested and seeded in fresh culture medium for an additional 72 h, cell proliferation resumed (right graph). Therefore, cell cycle arrest occurred after the cells were exposed to CuO-NPs.

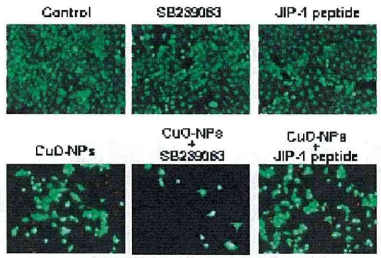

Figure S9. Effects of SB239063 and JNK interacting protein 1 (JIP-1), which are inhibitors of p38 and JNK, respectively. Double staining with calcein acetoxymethyl ester (calcein-AM) and propidium iodide (PI). SB239063 and CuO-NPs (CuO-NPs + SB239063) decreased the number of viable cells more than CuO-NPs alone. In the presence of SB239063, many cells that were exposed to CuO-NPs detached from the culture dish.

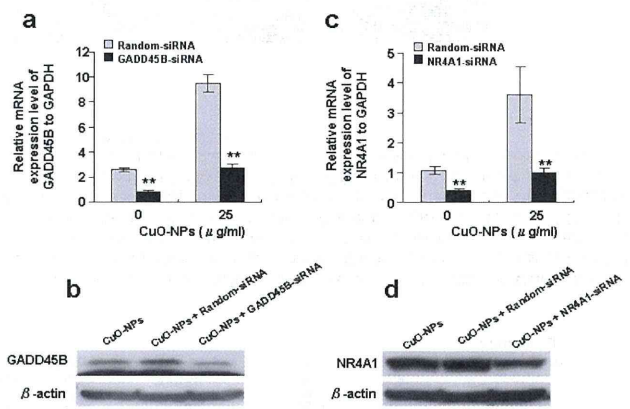

Figure S10. siRNA knockdown efficiency of *GADD45B* and *NR4A1*. (a) mRNA expression level of GADD45B. (b) Western blotting. The concentration of CuO-NPs was 25 μg/mL. GADD45B siRNA suppressed the expression at protein level. (c) mRNA expression level of NR4A1. (d) Western blotting. NR4A1 siRNA suppressed expression of NR4A1 at protein level.

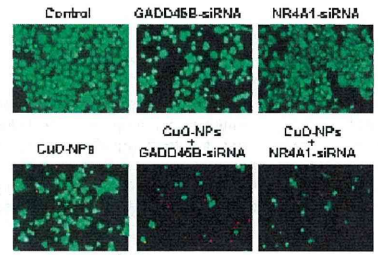

Figure S11. Effect of siRNA knockdown on the expression of *GADD45B* and *NR4A1* on the cytotoxicity of CuO-NPs. Double staining with calcein-AM and PI. Knockdown of *GADD45B* and *NR4A1* decreased the number of viable cells after cells were exposed to CuO-NPs. The number of dead cells as indicated by PI staining is not accurate because it included dead cells that detached from the surface of the culture dish.

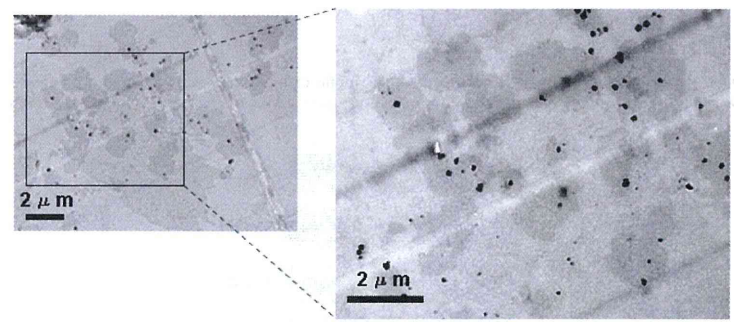

Figure S12. CuO-NPs in dead cell observed by TEM. Black dots indicate aggregates of CuO-NPs. Cells were cultured in medium with 25 μg/mL CuO-NPs for 24 h, and then dead cells detached from culture dish were harvested. Right panel is a magnified image of leaflet in left panel.

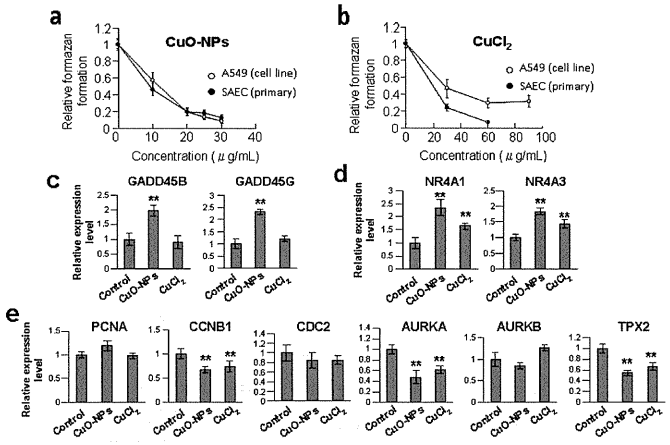

Figure S13. Cytotoxicity of CuO-NPs and Cu ions to primary human lung epithelial cells and change of gene expression. (a) Comparison of CuO-NPs toxicity between primary human epithelial cells (SAEC) and A549 cells. (b) Comparison of Cu ion toxicity between SAEC and A549 cells. (c-e) Expression level of genes in SAEC. Genes in (c) upregulated in CuO-NPs but not in 30 μ g/mL CuCl2 in A549 cells. SAEC cells showed similar pattern. Genes in (d) upregulated in both CuO-NPs and 30 μ g/mL CuCl2 in A549 cells. SAEC cells showed similar pattern. Genes in (e) downregulated in both CuO-NPs and 30 μ g/mL CuCl2 in A549 cells. SAEC cells showed similar pattern in CCNB1, AURKA and TPX2, but not PCNA, CDC2 and AURKB. For gene expression analysis, SAEC cells were exposed to media containing 25 μ g/mL CuO-NPs or 30 μ g/mL CuCl2 for 24 h.

Table S1. List of genes upregulated by CuO-NPs classified into the GO category of "Nucleobase, nucleoside, nucleotide and nucleic acid metabolic process". Fold-change is represented by logarithmic ratio (log_2 ratio) to expression level in control.

Gene name	Description	Fold- change (log_2 ratio)
ACRC	Homo sapiens acidic repeat containing (ACRC), mRNA [NM_052957]	2.82
AFF1	Homo sapiens AF4/FMR2 family, member 1 (AFF1), mRNA [NM_005935]	2.18
ALS2	Homo sapiens amyotrophic lateral sclerosis 2 (juvenile) (ALS2), transcript variant 2, mRNA [NM_001135745]	2.00
ARC	Homo sapiens activity-regulated cytoskeleton-associated protein (ARC), mRNA [NM_015193]	3.06
ATF1	Homo sapiens activating transcription factor 1 (ATF1), mRNA [NM_005171]	1.11
ATF3	Homo sapiens activating transcription factor 3 (ATF3), transcript variant 4, mRNA [NM_001040619]	4.22
ATP6V1A	Homo sapiens ATPase, H+ transporting, lysosomal 70kDa, V1 subunit A (ATP6V1A), mRNA [NM_001690]	1.34
ATP6V1B2	Homo sapiens ATPase, H+ transporting, lysosomal 56/58kDa, V1 subunit B2 (ATP6V1B2), mRNA [NM_001693]	1.23
ATP6V1C1	Homo sapiens ATPase, H+ transporting, lysosomal 42kDa, V1 subunit C1 (ATP6V1C1), mRNA [NM_001695]	2.31
ATP6V1D	Homo sapiens ATPase, H+ transporting, lysosomal 34kDa, V1 subunit D (ATP6V1D), mRNA [NM_015994]	1.85
ATP6V1G1	Homo sapiens ATPase, H+ transporting, lysosomal 13kDa, V1 subunit G1 (ATP6V1G1), mRNA [NM_004888]	1.49
ATP6V1H	Homo sapiens ATPase, H+ transporting, lysosomal 50/57kDa, V1 subunit H (ATP6V1H), transcript variant 1, mRNA [NM_015941]	1.26
BLOC1S1	Homo sapiens biogenesis of lysosomal organelles complex-1, subunit 1 (BLOC1S1), mRNA [NM_001487]	1.06
BRF2	Homo sapiens BRF2, subunit of RNA polymerase III transcription initiation factor, BRF1-like (BRF2), mRNA [NM_018310]	1.86
CARD6	Homo sapiens caspase recruitment domain family, member 6 (CARD6), mRNA [NM_032587]	1.10
CCNK	Homo sapiens cyclin K (CCNK), transcript variant 2, mRNA [NM_003858]	4.88
CDC40	Homo sapiens cell division cycle 40 homolog (S. cerevisiae) (CDC40), mRNA [NM_015891]	1.32
CDKN2AIP	Homo sapiens CDKN2A interacting protein (CDKN2AIP), mRNA [NM_017632]	1.18
CEBPG	Homo sapiens CCAAT/enhancer binding protein (C/EBP), gamma (CEBPG), mRNA [NM_001806]	1.09
CIR	Homo sapiens CBF1 interacting corepressor (CIR), mRNA [NM_004882]	1.21
CLU	Homo sapiens clusterin (CLU), transcript variant 2, mRNA [NM_203339]	1.24
CPEB4	Homo sapiens cytoplasmic polyadenylation element binding protein 4 (CPEB4), mRNA [NM_030627]	1.57
CREM	Homo sapiens cAMP responsive element modulator (CREM), transcript variant 19, mRNA [NM_183013]	1.15
CRIPT	Homo sapiens cysteine-rich PDZ-binding protein (CRIPT), mRNA [NM_014171]	1.73
CUGBP1	Homo sapiens CUG triplet repeat, RNA binding protein 1 (CUGBP1), transcript variant 2, mRNA [NM_198700]	1.65
DHX58	Homo sapiens DEXH (Asp-Glu-X-His) box polypeptide 58 (DHX58), mRNA [NM_024119]	2.22
E2F6	Homo sapiens E2F transcription factor 6 (E2F6), mRNA [NM_198256]	1.06
EGR1	Homo sapiens early growth response 1 (EGR1), mRNA [NM_001964]	3.89
ELL	Homo sapiens elongation factor RNA polymerase II (ELL), mRNA [NM_006532]	1.46
FBXL19	Homo sapiens F-box and leucine-rich repeat protein 19 (FBXL19), mRNA [NM_001099784]	1.46
FOS	Homo sapiens v-fos FBJ murine osteosarcoma viral oncogene homolog (FOS), mRNA [NM_005252]	4.48
FOSB	Homo sapiens FBJ murine osteosarcoma viral oncogene homolog B (FOSB), transcript variant 1, mRNA [NM_006732]	5.70
FOXN3	Homo sapiens forkhead box N3 (FOXN3), transcript variant 2, mRNA [NM_005197]	1.47
FSD1L	Homo sapiens fibronectin type III and SPRY domain containing 1-like (FSD1L), transcript variant 2, mRNA [NM_031919]	1.61
GABPA	Homo sapiens GA binding protein transcription factor, alpha subunit 60kDa (GABPA), mRNA [NM_002040]	2.89
GEM	Homo sapiens GTP binding protein overexpressed in skeletal muscle (GEM), transcript	1.60

	variant 1, mRNA [NM_005261]	
GRN	Homo sapiens granulin (GRN), mRNA [NM_002087]	1.08
GTF2B	Homo sapiens general transcription factor IIB (GTF2B), mRNA [NM_001514]	1.32
HBP1	Homo sapiens HMG-box transcription factor 1 (HBP1), mRNA [NM_012257]	2.84
HES1	Homo sapiens hairy and enhancer of split 1, (Drosophila) (HES1), mRNA [NM_005524]	1.52
HEY1	Homo sapiens hairy/enhancer-of-split related with YRPW motif 1 (HEY1), transcript variant 2, mRNA [NM_001040708]	1.22
HINT3	Homo sapiens histidine triad nucleotide binding protein 3 (HINT3), mRNA [NM_138571]	1.60
HIST1H2AM	Homo sapiens histone cluster 1, H2am (HIST1H2AM), mRNA [NM_003514]	1.42
HIST2H2AA4	Homo sapiens histone cluster 2, H2aa4 (HIST2H2AA4), mRNA [NM_001040874]	1.66
HIST2H2AB	Homo sapiens histone cluster 2, H2ab (HIST2H2AB), mRNA [NM_175065]	1.20
HNRNPH2	Homo sapiens heterogeneous nuclear ribonucleoprotein H2 (H') (HNRNPH2), transcript variant 1, mRNA [NM_019597]	1.42
HSF2	Homo sapiens heat shock transcription factor 2 (HSF2), transcript variant 1, mRNA [NM_004506]	1.28
HUS1	Homo sapiens HUS1 checkpoint homolog (S. pombe) (HUS1), mRNA [NM_004507]	1.32
ING4	Homo sapiens inhibitor of growth family, member 4 (ING4), transcript variant 1, mRNA [NM_016162]	1.54
ISG20	Homo sapiens interferon stimulated exonuclease gene 20kDa (ISG20), mRNA [NM_002201]	1.08
ISY1	Homo sapiens ISY1 splicing factor homolog (S. cerevisiae) (ISY1), mRNA [NM_020701]	1.11
JDP2	Homo sapiens Jun dimerization protein 2 (JDP2), transcript variant 1, mRNA [NM_130469]	1.13
KBTBD4	Homo sapiens kelch repeat and BTB (POZ) domain containing 4 (KBTBD4), transcript variant 2, mRNA [NM_016506]	1.48
KBTBD8	Homo sapiens kelch repeat and BTB (POZ) domain containing 8 (KBTBD8), mRNA [NM_032505]	1.97
KIAA1627	Homo sapiens KIAA1627 protein (KIAA1627), mRNA [NM_020961]	1.32
KLF7	Homo sapiens Kruppel-like factor 7 (ubiquitous) (KLF7), mRNA [NM_003709]	1.21
KLHL18	Homo sapiens kelch-like 18 (Drosophila), mRNA (cDNA clone IMAGE:4081125), partial cds. [BC015962]	1.16
LARP4	Homo sapiens La ribonucleoprotein domain family, member 4 (LARP4), transcript variant 2, mRNA [NM_199188]	1.76
LAT	Homo sapiens linker for activation of T cells (LAT), transcript variant 1, mRNA [NM_014387]	2.03
LATS2	Homo sapiens LATS, large tumor suppressor, homolog 2 (Drosophila) (LATS2), mRNA [NM_014572]	1.20
MAFF	Homo sapiens v-maf musculoaponeurotic fibrosarcoma oncogene homolog F (avian) (MAFF), transcript variant 1, mRNA [NM_012323]	2.26
MAFG	Homo sapiens v-maf musculoaponeurotic fibrosarcoma oncogene homolog G (avian) (MAFG), transcript variant 1, mRNA [NM_002359]	1.34
MAFK	Homo sapiens v-maf musculoaponeurotic fibrosarcoma oncogene homolog K (avian) (MAFK), mRNA [NM_002360]	1.55
MAGOH	Homo sapiens mago-nashi homolog, proliferation-associated (Drosophila) (MAGOH), mRNA [NM_002370]	1.18
MED13	Homo sapiens mediator complex subunit 13 (MED13), mRNA [NM_005121]	1.89
MED21	Homo sapiens mediator complex subunit 21 (MED21), mRNA [NM_004264]	1.12
MLXIPL	Homo sapiens MLX interacting protein-like (MLXIPL), transcript variant 1, mRNA [NM_032951]	1.73
MSI2	Homo sapiens musashi homolog 2 (Drosophila) (MSI2), transcript variant 2, mRNA [NM_170721]	1.52
MT1A	Homo sapiens metallothionein 1A (MT1A), mRNA [NM_005946]	2.19
MTF1	Homo sapiens metal-regulatory transcription factor 1 (MTF1), mRNA [NM_005955]	1.65
MXI1	Homo sapiens MAX interactor 1 (MXI1), transcript variant 2, mRNA [NM_130439]	1.77
MYNN	Homo sapiens myoneurin (MYNN), mRNA [NM_018657]	1.08
NAP1L5	Homo sapiens nucleosome assembly protein 1-like 5 (NAP1L5), mRNA [NM_153757]	1.01
NFATC1	Homo sapiens nuclear factor of activated T-cells, cytoplasmic, calcineurin-dependent 1 (NFATC1), transcript variant 1, mRNA [NM_172390]	1.83
NFIL3	Homo sapiens nuclear factor, interleukin 3 regulated (NFIL3), mRNA [NM_005384]	1.08

NR4A1	Homo sapiens nuclear receptor subfamily 4, group A, member 1 (NR4A1), transcript variant 1, mRNA [NM_002135]	5.28
NR4A3	Homo sapiens nuclear receptor subfamily 4, group A, member 3 (NR4A3), transcript variant 4, mRNA [NM_173199]	3.06
OGT	Homo sapiens O-linked N-acetylglucosamine (GlcNAc) transferase (UDP-N-acetylglucosamine:polypeptide-N-acetylglucosaminyl transferase) (OGT), transcript variant 1, mRNA [NM_181672]	1.38
PAIP2	Homo sapiens poly(A) binding protein interacting protein 2 (PAIP2), transcript variant 1, mRNA [NM_001033112]	1.12
PAPOLA	Homo sapiens poly(A) polymerase alpha (PAPOLA), mRNA [NM_032632]	1.60
PCF11	Homo sapiens PCF11, cleavage and polyadenylation factor subunit, homolog (S. cerevisiae) (PCF11), mRNA [NM_015885]	3.27
PHC3	Homo sapiens polyhomeotic homolog 3 (Drosophila) (PHC3), mRNA [NM_024947]	1.68
PHF1	Homo sapiens PHD finger protein 1 (PHF1), transcript variant 2, mRNA [NM_024165]	1.04
PHTF1	Homo sapiens putative homeodomain transcription factor 1 (PHTF1), mRNA [NM_006608]	1.39
PLRG1	Homo sapiens pleiotropic regulator 1 (PRL1 homolog, Arabidopsis) (PLRG1), mRNA [NM_002669]	1.38
PMS2L2	Homo sapiens postmeiotic segregation increased 2-like 2 pseudogene (PMS2L2), non-coding RNA [NR_003614]	1.02
PROP1	Homo sapiens PROP paired-like homeobox 1 (PROP1), mRNA [NM_006261]	1.95
PRPF18	Homo sapiens PRP18 pre-mRNA processing factor 18 homolog (S. cerevisiae) (PRPF18), mRNA [NM_003675]	1.43
RBBP6	Homo sapiens retinoblastoma binding protein 6 (RBBP6), transcript variant 1, mRNA [NM_006910]	1.10
RIOK3	Homo sapiens RIO kinase 3 (yeast) (RIOK3), mRNA [NM_003831]	2.38
RIT1	Homo sapiens Ras-like without CAAX 1 (RIT1), mRNA [NM_006912]	1.89
RLF	Homo sapiens rearranged L-myc fusion (RLF), mRNA [NM_012421]	1.44
RNF11	Homo sapiens ring finger protein 11 (RNF11), mRNA [NM_014372]	1.15
RNF12	Homo sapiens ring finger protein 12 (RNF12), transcript variant 1, mRNA [NM_016120]	1.68
RNF185	Homo sapiens ring finger protein 185 (RNF185), transcript variant 1, mRNA [NM_152267]	1.07
RNMT	Homo sapiens RNA (guanine-7-) methyltransferase (RNMT), mRNA [NM_003799]	1.27
RP2	Homo sapiens retinitis pigmentosa 2 (X-linked recessive) (RP2), mRNA [NM_006915]	1.35
RPUSD4	Homo sapiens RNA pseudouridylate synthase domain containing 4 (RPUSD4), mRNA [NM_032795]	1.06
RYBP	Homo sapiens RING1 and YY1 binding protein (RYBP), mRNA [NM_012234]	1.02
SBNO1	Homo sapiens cDNA FLJ23676 fis, clone HEP08548, highly similar to Homo sapiens mRNA for MOP-3. [AK074256]	1.19
SCML1	Homo sapiens sex comb on midleg-like 1 (Drosophila) (SCML1), transcript variant 1, mRNA [NM_001037540]	2.00
SIN3B	Homo sapiens SIN3 homolog B, transcription regulator (yeast), mRNA (cDNA clone IMAGE:3923074), partial cds. [BC025026]	1.28
SIRT6	Homo sapiens sirtuin (silent mating type information regulation 2 homolog) 6 (S. cerevisiae) (SIRT6), mRNA [NM_016539]	1.68
SLC25A44	Homo sapiens solute carrier family 25, member 44 (SLC25A44), transcript variant 1, mRNA [NM_014655]	1.12
SLU7	Homo sapiens SLU7 splicing factor homolog (S. cerevisiae) (SLU7), mRNA [NM_006425]	1.93
SNAI1	Homo sapiens snail homolog 1 (Drosophila) (SNAI1), mRNA [NM_005985]	3.18
SNIP1	Homo sapiens Smad nuclear interacting protein 1 (SNIP1), mRNA [NM_024700]	3.07
SOX8	Homo sapiens SRY (sex determining region Y)-box 8 (SOX8), mRNA [NM_014587]	1.93
SP1	Homo sapiens Sp1 transcription factor (SP1), transcript variant 1, mRNA [NM_138473]	2.03
SREBF2	Homo sapiens sterol regulatory element binding transcription factor 2 (SREBF2), mRNA [NM_004599]	1.32
SUPT4H1	Homo sapiens suppressor of Ty 4 homolog 1 (S. cerevisiae) (SUPT4H1), mRNA [NM_003168]	1.23
TAF13	Homo sapiens TAF13 RNA polymerase II, TATA box binding protein (TBP)-associated factor, 18kDa (TAF13), mRNA [NM_005645]	1.98
TAF7	Homo sapiens TAF7 RNA polymerase II, TATA box binding protein (TBP)-associated factor, 55kDa (TAF7), mRNA [NM_005642]	1.41

TAF8	Homo sapiens TAF8 RNA polymerase II, TATA box binding protein (TBP)-associated factor, 43kDa, mRNA (cDNA clone IMAGE:5166848), with apparent retained intron. [BC033728]	1.29
TDG	Homo sapiens thymine-DNA glycosylase (TDG), mRNA [NM_003211]	1.14
TEAD1	Homo sapiens TEA domain family member 1 (SV40 transcriptional enhancer factor) (TEAD1), mRNA [NM_021961]	1.30
TFIP11	Homo sapiens tuftelin interacting protein 11 (TFIP11), transcript variant 1, mRNA [NM_001008697]	1.28
THAP1	Homo sapiens THAP domain containing, apoptosis associated protein 1 (THAP1), transcript variant 1, mRNA [NM_018105]	1.16
TTF1	Homo sapiens transcription termination factor, RNA polymerase I (TTF1), mRNA [NM_007344]	1.00
UHMK1	Homo sapiens U2AF homology motif (UHM) kinase 1 (UHMK1), mRNA [NM_175866]	2.05
USP15	Homo sapiens ubiquitin specific peptidase 15 (USP15), mRNA [NM_006313]	1.33
USP32	Homo sapiens ubiquitin specific peptidase 32 (USP32), mRNA [NM_032582]	1.52
UTP11L	Homo sapiens UTP11-like, U3 small nucleolar ribonucleoprotein, (yeast) (UTP11L), mRNA [NM_016037]	1.28
ZBTB43	Homo sapiens zinc finger and BTB domain containing 43 (ZBTB43), transcript variant 1, mRNA [NM_014007]	1.89
ZBTB5	Homo sapiens zinc finger and BTB domain containing 5 (ZBTB5), mRNA [NM_014872]	1.43
ZNF10	Homo sapiens zinc finger protein 10 (ZNF10), mRNA [NM_015394]	2.81
ZNF12	Homo sapiens zinc finger protein 12 (ZNF12), transcript variant 1, mRNA [NM_016265]	1.00
ZNF121	Homo sapiens zinc finger protein 121 (ZNF121), mRNA [NM_001008727]	1.03
ZNF143	Homo sapiens zinc finger protein 143 (ZNF143), mRNA [NM_003442]	1.90
ZNF175	Homo sapiens zinc finger protein 175, mRNA (cDNA clone IMAGE:4301632), partial cds. [BC007778]	2.43
ZNF211	Homo sapiens zinc finger protein 211 (ZNF211), transcript variant 2, mRNA [NM_198855]	1.50
ZNF222	Homo sapiens zinc finger protein 222 (ZNF222), transcript variant 2, mRNA [NM_013360]	2.06
ZNF224	Homo sapiens cDNA FLJ78762 complete cds, highly similar to Homo sapiens zinc finger protein 224, mRNA. [AK292500]	1.61
ZNF236	Homo sapiens zinc finger protein 236 (ZNF236), mRNA [NM_007345]	1.02
ZNF256	Homo sapiens zinc finger protein 256 (ZNF256), mRNA [NM_005773]	1.65
ZNF257	Homo sapiens zinc finger protein 257 (ZNF257), mRNA [NM_033468]	1.47
ZNF266	Homo sapiens zinc finger protein 266 (ZNF266), mRNA [NM_006631]	1.12
ZNF274	Homo sapiens zinc finger protein 274 (ZNF274), transcript variant ZNF274c, mRNA [NM_133502]	1.19
ZNF277	Homo sapiens zinc finger protein 277 (ZNF277), mRNA [NM_021994]	1.17
ZNF286A	Homo sapiens zinc finger protein 286A (ZNF286A), transcript variant 1, mRNA [NM_020652]	2.20
ZNF324	Homo sapiens zinc finger protein 324 (ZNF324), mRNA [NM_014347]	1.09
ZNF331	Homo sapiens zinc finger protein 331 (ZNF331), transcript variant 1, mRNA [NM_018555]	1.48
ZNF34	Homo sapiens zinc finger protein 34 (ZNF34), mRNA [NM_030580]	1.40
ZNF37A	Homo sapiens zinc finger protein 37A (ZNF37A), transcript variant 1, mRNA [NM_001007094]	1.09
ZNF383	Homo sapiens zinc finger protein 383 (ZNF383), mRNA [NM_152604]	1.08
ZNF394	Homo sapiens zinc finger protein 394 (ZNF394), mRNA [NM_032164]	1.35
ZNF436	Homo sapiens zinc finger protein 436 (ZNF436), transcript variant 1, mRNA [NM_001077195]	1.76
ZNF461	Homo sapiens zinc finger protein 461 (ZNF461), mRNA [NM_153257]	1.68
ZNF473	Homo sapiens zinc finger protein 473 (ZNF473), transcript variant 1, mRNA [NM_015428]	1.92
ZNF484	Homo sapiens zinc finger protein 484 (ZNF484), transcript variant 2, mRNA [NM_001007101]	1.16
ZNF507	Homo sapiens zinc finger protein 507 (ZNF507), transcript variant 2, mRNA [NM_014910]	1.19
ZNF512	Homo sapiens zinc finger protein 512 (ZNF512), mRNA [NM_032434]	1.19
ZNF550	Homo sapiens zinc finger protein 550, mRNA (cDNA clone IMAGE:6044705). [BC053858]	1.04
ZNF557	Homo sapiens zinc finger protein 557 (ZNF557), transcript variant 1, mRNA [NM_024341]	1.78

ZNF558	Homo sapiens zinc finger protein 558 (ZNF558), mRNA [NM_144693]	1.05
ZNF565	Homo sapiens zinc finger protein 565 (ZNF565), transcript variant 1, mRNA [NM_001042474]	1.23
ZNF625	Homo sapiens zinc finger protein 625 (ZNF625), mRNA [NM_145233]	1.20
ZNF626	Homo sapiens zinc finger protein 626 (ZNF626), transcript variant 2, mRNA [NM_145297]	1.31
ZNF669	Homo sapiens zinc finger protein 669 (ZNF669), transcript variant 1, mRNA [NM_024804]	3.33
ZNF707	Homo sapiens zinc finger protein 707 (ZNF707), transcript variant 1, mRNA [NM_173831]	1.63
ZNF721	Homo sapiens zinc finger protein 721 (ZNF721), mRNA [NM_133474]	1.17
ZNF780B	Homo sapiens zinc finger protein 780B (ZNF780B), mRNA [NM_001005851]	1.14
ZNF79	Homo sapiens zinc finger protein 79 (ZNF79), mRNA [NM_007135]	1.08
ZNF8	Homo sapiens zinc finger protein 8 (ZNF8), mRNA [NM_021089]	2.14
ZRANB2	Homo sapiens zinc finger, RAN-binding domain containing 2 (ZRANB2), transcript variant 1, mRNA [NM_203350]	2.14
ZRSR2	Homo sapiens zinc finger (CCCH type), RNA-binding motif and serine/arginine rich 2 (ZRSR2), mRNA [NM_005089]	1.42
ZSCAN2	Homo sapiens zinc finger and SCAN domain containing 2 (ZSCAN2), transcript variant 2, mRNA [NM_017894]	1.12
ZSCAN20	Homo sapiens zinc finger and SCAN domain containing 20 (ZSCAN20), mRNA [NM_145238]	1.05

Table S2. List of genes upregulated by CuO-NPs classified into the GO category of "response to stress". Fold-change is represented by logarithmic ratio (log_2 ratio) to expression level in control.

Gene name	Description	Fold-change (log_2 ratio)
ATF1	Homo sapiens activating transcription factor 1 (ATF1), mRNA [NM_005171]	1.11
CDKL3	Homo sapiens cyclin-dependent kinase-like 3 (CDKL3), transcript variant 2, mRNA [NM_016508]	2.37
CLK1	Homo sapiens CDC-like kinase 1 (CLK1), mRNA [NM_004071]	2.18
CREM	Homo sapiens cAMP responsive element modulator (CREM), transcript variant 19, mRNA [NM_183013]	1.15
CRYAB	Homo sapiens crystallin, alpha B (CRYAB), mRNA [NM_001885]	4.36
DNAJA1	Homo sapiens DnaJ (Hsp40) homolog, subfamily A, member 1 (DNAJA1), mRNA [NM_001539]	1.33
DNAJA4	Homo sapiens PRO1472 mRNA, complete cds. [AF116663]	5.65
DNAJB1	Homo sapiens DnaJ (Hsp40) homolog, subfamily B, member 1 (DNAJB1), mRNA [NM_006145]	2.94
DNAJB6	Homo sapiens DnaJ (Hsp40) homolog. subfamily B, member 6 (DNAJB6), transcript variant 1. mRNA [NM_058246]	2.17
DNAJB9	Homo sapiens DnaJ (Hsp40) homolog. subfamily B, member 9 (DNAJB9), mRNA [NM_012328]	1.55
DNAJC3	Homo sapiens DnaJ (Hsp40) homolog, subfamily C, member 3. mRNA (cDNA clone IMAGE:5218144), with apparent retained intron. [BC033823]	1.60
FOS	Homo sapiens v-fos FBJ murine osteosarcoma viral oncogene homolog (FOS), mRNA [NM_005252]	4.48
FOSB	Homo sapiens FBJ murine osteosarcoma viral oncogene homolog B (FOSB), transcript variant 1, mRNA [NM_006732]	5.70
FSD1L	Homo sapiens fibronectin type III and SPRY domain containing 1-like (FSD1L), transcript variant 2, mRNA [NM_031919]	1.61
GADD45B	Homo sapiens growth arrest and DNA-damage-inducible, beta (GADD45B), mRNA [NM_015675]	2.96
GADD45G	Homo sapiens growth arrest and DNA-damage-inducible, gamma (GADD45G), mRNA [NM_006705]	3.59
HRH1	Homo sapiens histamine receptor H1 (HRH1), transcript variant 4, mRNA [NM_000861]	1.00
HSF2	Homo sapiens heat shock transcription factor 2 (HSF2), transcript variant 1, mRNA [NM_004506]	1.28
HSP90AA1	Homo sapiens heat shock protein 90kDa alpha (cytosolic), class A member 1 (HSP90AA1), transcript variant 2, mRNA [NM_005348]	1.20
HSPA13	Homo sapiens heat shock protein 70kDa family, member 13 (HSPA13), mRNA [NM_006948]	1.10
HSPA6	Homo sapiens heat shock 70kDa protein 6 (HSP70B') (HSPA6), mRNA [NM_002155]	4.67
HSPB8	Homo sapiens heat shock 22kDa protein 8 (HSPB8), mRNA [NM_014365]	1.99
HSPH1	Homo sapiens heat shock 105kDa/110kDa protein 1 (HSPH1), mRNA [NM_006644]	2.06
JDP2	Homo sapiens Jun dimerization protein 2 (JDP2), transcript variant 1, mRNA [NM_130469]	1.13
NLK	Homo sapiens nemo-like kinase (NLK), mRNA [NM_016231]	1.32
NR4A1	Homo sapiens nuclear receptor subfamily 4, group A, member 1 (NR4A1), transcript variant 1, mRNA [NM_002135]	5.28
NR4A3	Homo sapiens nuclear receptor subfamily 4, group A, member 3 (NR4A3), transcript variant 4, mRNA [NM_173199]	3.06
ST13	Homo sapiens suppression of tumorigenicity 13 (colon carcinoma) (Hsp70 interacting protein) (ST13), mRNA [NM_003932]	1.07
TTC1	Homo sapiens tetratricopeptide repeat domain 1 (TTC1), mRNA [NM_003314]	1.32
VEGFA	Homo sapiens vascular endothelial growth factor A (VEGFA), transcript variant 1, mRNA [NM_001025366]	1.24

Table S3. List of genes downregulated by CuO-NPs classified into the GO category of "cell cycle". Fold-change is represented by logarithmic ratio (log_2 ratio) to expression level in control. *, also classified into the category of "mitosis".

Gene name	Description	Fold-change (log_2 ratio)
ACTR3B*	Homo sapiens ARP3 actin-related protein 3 homolog B (yeast) (ACTR3B), transcript variant 2, mRNA [NM_001040135]	-1.07
ATR	Homo sapiens ataxia telangiectasia and Rad3 related (ATR), mRNA [NM_001184]	-1.11
AURKA*	Homo sapiens aurora kinase A (AURKA), transcript variant 1, mRNA [NM_198433]	-1.21
AURKB*	Homo sapiens aurora kinase B (AURKB), mRNA [NM_004217]	-1.13
AXL	Homo sapiens AXL receptor tyrosine kinase (AXL), transcript variant 1, mRNA [NM_021913]	-1.81
BCL2A1	Homo sapiens BCL2-related protein A1 (BCL2A1), transcript variant 1, mRNA [NM_004049]	-1.11
CCNA2*	Homo sapiens cyclin A2 (CCNA2), mRNA [NM_001237]	-1.39
CCNB1*	Homo sapiens cyclin B1 (CCNB1), mRNA [NM_031966]	-1.74
CCNB2*	Homo sapiens cyclin B2 (CCNB2), mRNA [NM_004701]	-1.44
CDC2*	Homo sapiens cell division cycle 2, G1 to S and G2 to M (CDC2), transcript variant 1, mRNA [NM_001786]	-1.41
CDC20	Homo sapiens cell division cycle 20 homolog (S. cerevisiae) (CDC20), mRNA [NM_001255]	-1.23
CDK6*	Homo sapiens cyclin-dependent kinase 6 (CDK6), mRNA [NM_001259]	-1.28
CDKN1B	Homo sapiens cyclin-dependent kinase inhibitor 1B (p27, Kip1) (CDKN1B), mRNA [NM_004064]	-1.30
CDKN2C	Homo sapiens cyclin-dependent kinase inhibitor 2C (p18, inhibits CDK4) (CDKN2C), transcript variant 2, mRNA [NM_078626]	-1.57
CIT*	Homo sapiens citron (rho-interacting, serine/threonine kinase 21) (CIT), mRNA [NM_007174]	-1.82
CKAP5	Homo sapiens cytoskeleton associated protein 5 (CKAP5), transcript variant 1, mRNA [NM_001008938]	-1.07
DBF4	Homo sapiens DBF4 homolog (S. cerevisiae) (DBF4), mRNA [NM_006716]	-1.37
DIS3L*	Homo sapiens DIS3 mitotic control homolog (S. cerevisiae)-like (DIS3L), transcript variant 2, mRNA [NM_133375]	-1.71
DLC1	Homo sapiens deleted in liver cancer 1 (DLC1), transcript variant 1, mRNA [NM_182643]	-1.09
DNAJC5	full-length cDNA clone CS0DN003YL17 of Adult brain of Homo sapiens (human). [CR607484]	-1.38
DST	Homo sapiens cDNA: FLJ21489 fis, clone COL05450. [AK025142]	-1.03
E2F7	Homo sapiens E2F transcription factor 7 (E2F7), mRNA [NM_203394]	-1.28
E2F8	Homo sapiens E2F transcription factor 8 (E2F8), mRNA [NM_024680]	-1.61
EFHB	Homo sapiens EF-hand domain family, member B (EFHB), mRNA [NM_144715]	-1.56
EIF2AK4	Homo sapiens eukaryotic translation initiation factor 2 alpha kinase 4 (EIF2AK4), mRNA [NM_001013703]	-1.17
EPHB2	Homo sapiens EPH receptor B2 (EPHB2), transcript variant 2, mRNA [NM_004442]	-1.28
ERBB2	Homo sapiens v-erb-b2 erythroblastic leukemia viral oncogene homolog 2, neuro/glioblastoma derived oncogene homolog (avian) (ERBB2), transcript variant 2, mRNA [NM_001005862]	-1.33
FBXL4	Homo sapiens F-box and leucine-rich repeat protein 4 (FBXL4), mRNA [NM_012160]	-1.09
FKBP7	Homo sapiens FK506 binding protein 7 (FKBP7), transcript variant 1, mRNA [NM_181342]	-1.06
FOXF2	Homo sapiens forkhead box F2 (FOXF2), mRNA [NM_001452]	-1.14
GPSM2*	Homo sapiens G-protein signaling modulator 2 (AGS3-like, C. elegans) (GPSM2), mRNA [NM_013296]	-1.19
GTSE1	Homo sapiens G-2 and S-phase expressed 1 (GTSE1), mRNA [NM_016426]	-1.42
JUB*	Homo sapiens jub, ajuba homolog (Xenopus laevis) (JUB), transcript variant 1, mRNA [NM_032876]	-1.41
KIAA1274	Homo sapiens KIAA1274 (KIAA1274), mRNA [NM_014431]	-1.14
KIAA1804	Homo sapiens mixed lineage kinase 4 (KIAA1804), mRNA [NM_032435]	-1.37
KIF18A*	Homo sapiens kinesin family member 18A (KIF18A), mRNA [NM_031217]	-1.17
KIF18B*	Homo sapiens hypothetical protein LOC146909, mRNA (cDNA clone IMAGE:4418755), partial cds. [BC048263]	-2.07
KIF20A*	Homo sapiens kinesin family member 20A (KIF20A), mRNA [NM_005733]	-2.05

KIF23*	Homo sapiens kinesin family member 23 (KIF23), transcript variant 1, mRNA [NM_138555]	-1.56
KIFC1*	Homo sapiens kinesin family member C1 (KIFC1), mRNA [NM_002263]	-1.26
MCM4	Homo sapiens minichromosome maintenance complex component 4 (MCM4), transcript variant 1, mRNA [NM_005914]	-1.09
MCM6	Homo sapiens minichromosome maintenance complex component 6 (MCM6), mRNA [NM_005915]	-1.10
MELK	Homo sapiens maternal embryonic leucine zipper kinase (MELK), mRNA [NM_014791]	-1.11
MOBKL2B*	Homo sapiens MOB1, Mps One Binder kinase activator-like 2B (yeast) (MOBKL2B), mRNA [NM_024761]	-1.11
MYBBP1A	Homo sapiens MYB binding protein (P160) 1a (MYBBP1A), transcript variant 2, mRNA [NM_014520]	-1.02
MYBL1	Homo sapiens v-myb myeloblastosis viral oncogene homolog (avian)-like 1 (MYBL1), mRNA [NM_001080416]	-1.84
MYC	Homo sapiens v-myc myelocytomatosis viral oncogene homolog (avian) (MYC), mRNA [NM_002467]	-1.48
MYH9*	Homo sapiens myosin, heavy chain 9, non-muscle (MYH9), mRNA [NM_002473]	-1.21
MYO5C*	Homo sapiens myosin VC (MYO5C), mRNA [NM_018728]	-1.39
NCAPD2*	Homo sapiens non-SMC condensin I complex, subunit D2 (NCAPD2), mRNA [NM_014865]	-1.12
NDC80	Homo sapiens NDC80 homolog, kinetochore complex component (S. cerevisiae) (NDC80), mRNA [NM_006101]	-1.01
NR2F2	Homo sapiens nuclear receptor subfamily 2, group F, member 2 (NR2F2), mRNA [NM_021005]	-1.11
NUF2*	Homo sapiens NUF2, NDC80 kinetochore complex component, homolog (S. cerevisiae) (NUF2), transcript variant 1, mRNA [NM_145697]	-1.17
OTUD4*	Homo sapiens OTU domain containing 4 (OTUD4), transcript variant 1, mRNA [NM_199324]	-1.47
PARP4	Homo sapiens poly (ADP-ribose) polymerase family, member 4 (PARP4), mRNA [NM_006437]	-1.18
PCNA	Homo sapiens proliferating cell nuclear antigen (PCNA), transcript variant 1, mRNA [NM_002592]	-1.37
PDGFA	Homo sapiens platelet-derived growth factor alpha polypeptide (PDGFA), transcript variant 1, mRNA [NM_002607]	-1.04
PLK2	Homo sapiens polo-like kinase 2 (Drosophila) (PLK2), mRNA [NM_006622]	-1.29
PMS1	Homo sapiens PMS1 postmeiotic segregation increased 1 (S. cerevisiae) (PMS1), transcript variant 1, mRNA [NM_000534]	-1.66
POLI*	Homo sapiens polymerase (DNA directed) iota (POLI), mRNA [NM_007195]	-1.58
PSKH1*	Homo sapiens protein serine kinase H1 (PSKH1), mRNA [NM_006742]	-1.28
PSRC1	Homo sapiens proline/serine-rich coiled-coil 1 (PSRC1), transcript variant 1, mRNA [NM_032636]	-1.61
PTPN13	Homo sapiens protein tyrosine phosphatase, non-receptor type 13 (APO-1/CD95 (Fas)-associated phosphatase) (PTPN13), transcript variant 4, mRNA [NM_080685]	-1.77
PTTG1*	Homo sapiens pituitary tumor-transforming 1 (PTTG1), mRNA [NM_004219]	-1.04
RAPGEF6*	Homo sapiens Rap guanine nucleotide exchange factor (GEF) 6 (RAPGEF6), mRNA [NM_016340]	-1.08
RBBP8	Homo sapiens retinoblastoma binding protein 8 (RBBP8), transcript variant 1, mRNA [NM_002894]	-1.31
ROR1	Tyrosine-protein kinase transmembrane receptor ROR1 Precursor (EC 2.7.10.1)(Neurotrophic tyrosine kinase, receptor-related 1) [Source:UniProtKB/Swiss-Prot;Acc:Q01973] [ENST00000371079]	-1.43
SASS6*	Homo sapiens spindle assembly 6 homolog (C. elegans) (SASS6), mRNA [NM_194292]	-1.07
SPTBN1	Homo sapiens spectrin, beta, non-erythrocytic 1 (SPTBN1), transcript variant 1, mRNA [NM_003128]	-1.21
SRGAP2	Homo sapiens SLIT-ROBO Rho GTPase activating protein 2 (SRGAP2), transcript variant 1, mRNA [NM_015326]	-1.17
TNS3	Homo sapiens tensin 3 (TNS3), mRNA [NM_022748]	-1.98
TOP2A*	Homo sapiens topoisomerase (DNA) II alpha 170kDa (TOP2A), mRNA [NM_001067]	-2.00
TPX2*	Homo sapiens TPX2, microtubule-associated, homolog (Xenopus laevis) (TPX2), mRNA [NM_012112]	-1.25
TRAF7	Homo sapiens TNF receptor-associated factor 7 (TRAF7), mRNA [NM_032271]	-1.01
TRIM14	Homo sapiens tripartite motif-containing 14 (TRIM14), transcript variant 1, mRNA [NM_014788]	-1.87
TRIM59	Homo sapiens tripartite motif-containing 59 (TRIM59), mRNA [NM_173084]	-1.86
TRIM6	Homo sapiens tripartite motif-containing 6 (TRIM6), transcript variant 1, mRNA [NM_001003818]	-1.64
TUBA3D*	Homo sapiens tubulin, alpha 3d (TUBA3D), mRNA [NM_080386]	-1.20
TUBB2B*	Homo sapiens tubulin, beta 2B (TUBB2B), mRNA [NM_178012]	-1.07
TUBB6*	Homo sapiens tubulin, beta 6 (TUBB6), mRNA [NM_032525]	-1.21
UBE2T*	Homo sapiens ubiquitin-conjugating enzyme E2T (putative) (UBE2T), mRNA [NM_014176]	-1.14
UHRF1	Homo sapiens ubiquitin-like with PHD and ring finger domains 1 (UHRF1), transcript variant 2, mRNA [NM_013282]	-1.37
UTRN	Homo sapiens utrophin (UTRN), mRNA [NM_007124]	-1.01
YWHAH	Homo sapiens tyrosine 3-monooxygenase/tryptophan 5-monooxygenase activation protein, eta polypeptide (YWHAH), mRNA [NM_003405]	-1.34
ZFP36L1*	Homo sapiens zinc finger protein 36, C3H type-like 1 (ZFP36L1), mRNA [NM_004926]	-1.45
ZFP36L2*	Homo sapiens zinc finger protein 36, C3H type-like 2 (ZFP36L2), mRNA [NM_006887]	-1.22

Table S4. List of genes downregulated by CuO-NPs classified into the GO category of "cytokinesis". Fold-change is represented by logarithmic ratio (log_2 ratio) to expression level in control.

Gene name	Description	Fold-change (log_2 ratio)
ACTR3B	Homo sapiens ARP3 actin-related protein 3 homolog B (yeast) (ACTR3B), transcript variant 2, mRNA [NM_001040135]	-1.069
AURKA	Homo sapiens aurora kinase A (AURKA), transcript variant 1, mRNA [NM_198433]	-1.206
AURKB	Homo sapiens aurora kinase B (AURKB), mRNA [NM_004217]	-1.129
CIT	Homo sapiens citron (rho-interacting, serine/threonine kinase 21) (CIT), mRNA [NM_007174]	-1.821
GPSM2	Homo sapiens G-protein signaling modulator 2 (AGS3-like, C. elegans) (GPSM2), mRNA [NM_013296]	-1.185
KIF18A	Homo sapiens kinesin family member 18A (KIF18A), mRNA [NM_031217]	-1.165
KIF18B	Homo sapiens hypothetical protein LOC146909, mRNA (cDNA clone IMAGE:4418755), partial cds. [BC048263]	-2.068
KIF20A	Homo sapiens kinesin family member 20A (KIF20A), mRNA [NM_005733]	-2.049
KIF20B	Homo sapiens kinesin family member 20B (KIF20B), mRNA [NM_016195]	-1.253
KIF23	Homo sapiens kinesin family member 23 (KIF23), transcript variant 1, mRNA [NM_138555]	-1.562
KIFC1	Homo sapiens kinesin family member C1 (KIFC1), mRNA [NM_002263]	-1.264
MOBKL2B	Homo sapiens MOB1, Mps One Binder kinase activator-like 2B (yeast) (MOBKL2B), mRNA [NM_024761]	-1.112
MYH9	Homo sapiens myosin, heavy chain 9, non-muscle (MYH9), mRNA [NM_002473]	-1.213
MYO5C	Homo sapiens myosin VC (MYO5C), mRNA [NM_018728]	-1.393
PSKH1	Homo sapiens protein serine kinase H1 (PSKH1), mRNA [NM_006742]	-1.281
PTPN13	Homo sapiens protein tyrosine phosphatase, non-receptor type 13 (APO-1/CD95 (Fas)-associated phosphatase) (PTPN13), transcript variant 4, mRNA [NM_080685]	-1.774

Table S5. List of genes downregulated by CuO-NPs classified into the GO category of "chromosome segregation". Fold-change is represented by logarithmic ratio (log_2 ratio) to expression level in control.

Gene name	Description	Fold-change (log_2 ratio)
KIF18A	Homo sapiens kinesin family member 18A (KIF18A), mRNA [NM_031217]	-1.17
KIF18B	Homo sapiens hypothetical protein LOC146909, mRNA (cDNA clone IMAGE:4418755), partial cds. [BC048263]	-2.07
KIF20A	Homo sapiens kinesin family member 20A (KIF20A), mRNA [NM_005733]	-2.05
KIF20B	Homo sapiens kinesin family member 20B (KIF20B), mRNA [NM_016195]	-1.25
KIF23	Homo sapiens kinesin family member 23 (KIF23), transcript variant 1, mRNA [NM_138555]	-1.56
KIFC1	Homo sapiens kinesin family member C1 (KIFC1), mRNA [NM_002263]	-1.26
NUF2	Homo sapiens NUF2, NDC80 kinetochore complex component, homolog (S. cerevisiae) (NUF2), transcript variant 1, mRNA [NM_145697]	-1.17
OTUD4	Homo sapiens OTU domain containing 4 (OTUD4), transcript variant 1, mRNA [NM_199324]	-1.47
POLI	Homo sapiens polymerase (DNA directed) iota (POLI), mRNA [NM_007195]	-1.58
PTTG1	Homo sapiens pituitary tumor-transforming 1 (PTTG1), mRNA [NM_004219]	-1.04
SASS6	Homo sapiens spindle assembly 6 homolog (C. elegans) (SASS6), mRNA [NM_194292]	-1.07
TOP2A	Homo sapiens topoisomerase (DNA) II alpha 170kDa (TOP2A), mRNA [NM_001067]	-2.00
TPX2	Homo sapiens TPX2, microtubule-associated, homolog (Xenopus laevis) (TPX2), mRNA [NM_012112]	-1.25
TUBA3D	Homo sapiens tubulin, alpha 3d (TUBA3D), mRNA [NM_080386]	-1.20
TUBB2B	Homo sapiens tubulin, beta 2B (TUBB2B), mRNA [NM_178012]	-1.07
TUBB6	Homo sapiens tubulin, beta 6 (TUBB6), mRNA [NM_032525]	-1.21
UBE2T	Homo sapiens ubiquitin-conjugating enzyme E2T (putative) (UBE2T), mRNA [NM_014176]	-1.14

Table S6. List of genes upregulated by CuO-NPs classified into the GO category of "cellular component organization". Fold-change is represented by logarithmic ratio (log_2 ratio) to expression level in control. *, Also classified into the category of "cellular component morphogenesis"

Gene name	Description	Fold-change (log_2 ratio)
ACTR3B*	Homo sapiens ARP3 actin-related protein 3 homolog B (yeast) (ACTR3B), transcript variant 2, mRNA [NM_001040135]	-1.07
ANGPTL4*	Homo sapiens angiopoietin-like 4 (ANGPTL4), transcript variant 1, mRNA [NM_139314]	-1.09
ATR	Homo sapiens ataxia telangiectasia and Rad3 related (ATR), mRNA [NM_001184]	-1.11
ATRX	Homo sapiens alpha thalassemia/mental retardation syndrome X-linked (RAD54 homolog, S. cerevisiae) (ATRX), transcript variant 1, mRNA [NM_000489]	-1.04
CENPA	Homo sapiens centromere protein A (CENPA), transcript variant 1, mRNA [NM_001809]	-1.80
CIT*	Homo sapiens citron (rho-interacting, serine/threonine kinase 21) (CIT), mRNA [NM_007174]	-1.82
CKAP5*	Homo sapiens cytoskeleton associated protein 5 (CKAP5), transcript variant 1, mRNA [NM_001008938]	-1.07
CLDN23*	Homo sapiens claudin 23 (CLDN23), mRNA [NM_194284]	-1.11
COCH*	Homo sapiens coagulation factor C homolog, cochlin (Limulus polyphemus) (COCH), transcript variant 2, mRNA [NM_004086]	-1.05
COL4A1*	Homo sapiens collagen, type IV, alpha 1 (COL4A1), mRNA [NM_001845]	-1.01
COL5A1*	Homo sapiens collagen, type V, alpha 1 (COL5A1), mRNA [NM_000093]	-1.30
COL5A2*	Homo sapiens collagen, type V, alpha 2 (COL5A2), mRNA [NM_000393]	-1.03
DAPK1*	Homo sapiens death-associated protein kinase 1 (DAPK1), mRNA [NM_004938]	-1.44
DLC1*	Homo sapiens deleted in liver cancer 1 (DLC1), transcript variant 1, mRNA [NM_182643]	-1.09
DLG5*	Homo sapiens discs, large homolog 5 (Drosophila) (DLG5), mRNA [NM_004747]	-1.36
DST*	Homo sapiens cDNA: FLJ21489 fis, clone COL05450. [AK025142]	-1.03
EHMT1	Homo sapiens euchromatic histone-lysine N-methyltransferase 1 (EHMT1), mRNA [NM_024757]	-1.18
EVI5*	Homo sapiens ecotropic viral integration site 5 (EVI5), mRNA [NM_005665]	-1.08
FOXF2*	Homo sapiens forkhead box F2 (FOXF2), mRNA [NM_001452]	-1.14
GEMIN5	Homo sapiens gem (nuclear organelle) associated protein 5 (GEMIN5), mRNA [NM_015465]	-1.59
GTSE1*	Homo sapiens G-2 and S-phase expressed 1 (GTSE1), mRNA [NM_016426]	-1.42
H1FX	Homo sapiens H1 histone family, member X (H1FX), mRNA [NM_006026]	-1.52
H2AFX	Homo sapiens H2A histone family, member X (H2AFX), mRNA [NM_002105]	-1.16
HMGB2	Homo sapiens high-mobility group box 2 (HMGB2), transcript variant 1, mRNA [NM_002129]	-2.06
IPP*	Homo sapiens intracisternal A particle-promoted polypeptide (IPP), mRNA [NM_005897]	-1.05
JUB*	Homo sapiens jub, ajuba homolog (Xenopus laevis) (JUB), transcript variant 1, mRNA [NM_032876]	-1.41
KIAA1804*	Homo sapiens mixed lineage kinase 4 (KIAA1804), mRNA [NM_032435]	-1.37
KIF18A*	Homo sapiens kinesin family member 18A (KIF18A), mRNA [NM_031217]	-1.17
KIF18B*	Homo sapiens hypothetical protein LOC146909, mRNA (cDNA clone IMAGE:4418755), partial cds. [BC048263]	-2.07
KIF20A*	Homo sapiens kinesin family member 20A (KIF20A), mRNA [NM_005733]	-2.05
KIF20B	Homo sapiens kinesin family member 20B (KIF20B), mRNA [NM_016195]	-1.25
KIF23*	Homo sapiens kinesin family member 23 (KIF23), transcript variant 1, mRNA [NM_138555]	-1.56
KIFC1*	Homo sapiens kinesin family member C1 (KIFC1), mRNA [NM_002263]	-1.26
KLHDC5*	Homo sapiens kelch domain containing 5 (KLHDC5), mRNA [NM_020782]	-1.43
LIMK2*	Homo sapiens LIM domain kinase 2 (LIMK2), transcript variant 2b, mRNA [NM_016733]	-1.18
LMNB1*	Homo sapiens lamin B1 (LMNB1), mRNA [NM_005573]	-2.04
LMNB2*	Homo sapiens lamin B2 (LMNB2), mRNA [NM_032737]	-1.71
MELK*	Homo sapiens maternal embryonic leucine zipper kinase (MELK), mRNA [NM_014791]	-1.11
MESDC1*	Homo sapiens mesoderm development candidate 1 (MESDC1), mRNA [NM_022566]	-1.01
MYO1B*	Homo sapiens myosin IB (MYO1B), transcript variant 2, mRNA [NM_012223]	-1.30
MYO5C*	Homo sapiens myosin VC (MYO5C), mRNA [NM_018728]	-1.39

NCAPD2	Homo sapiens non-SMC condensin I complex, subunit D2 (NCAPD2), mRNA [NM_014865]	-1.12
OBSL1*	Homo sapiens obscurin-like 1 (OBSL1), mRNA [NM_015311]	-1.11
OLFML2A*	Homo sapiens olfactomedin-like 2A (OLFML2A), mRNA [NM_182487]	-1.15
PCDH9*	Homo sapiens protocadherin 9 (PCDH9), transcript variant 1, mRNA [NM_203487]	-1.43
PDGFA*	Homo sapiens platelet-derived growth factor alpha polypeptide (PDGFA), transcript variant 1, mRNA [NM_002607]	-1.04
PODXL*	Homo sapiens podocalyxin-like (PODXL), transcript variant 1, mRNA [NM_001018111]	-1.69
PSKH1*	Homo sapiens protein serine kinase H1 (PSKH1), mRNA [NM_006742]	-1.28
PSRC1*	Homo sapiens proline/serine-rich coiled-coil 1 (PSRC1), transcript variant 1, mRNA [NM_032636]	-1.61
SASS6	Homo sapiens spindle assembly 6 homolog (C. elegans) (SASS6), mRNA [NM_194292]	-1.07
SETBP1	Homo sapiens SET binding protein 1 (SETBP1), transcript variant 1, mRNA [NM_015559]	-1.04
SIM2	Homo sapiens single-minded homolog 2 (Drosophila) (SIM2), transcript variant SIM2, mRNA [NM_005069]	-1.41
SPTBN1*	Homo sapiens spectrin, beta, non-erythrocytic 1 (SPTBN1), transcript variant 1, mRNA [NM_003128]	-1.21
TBC1D9B*	Homo sapiens TBC1 domain family, member 9B (with GRAM domain) (TBC1D9B), transcript variant 1, mRNA [NM_198868]	-1.08
THSD7A*	Homo sapiens cDNA FLJ11022 fis, clone PLACE1003771. [AK001884]	-1.39
TPM1*	Homo sapiens tropomyosin 1 (alpha) (TPM1), transcript variant 5, mRNA [NM_000366]	-1.09
TRIOBP*	Homo sapiens TRIO and F-actin binding protein (TRIOBP), transcript variant 6, mRNA [NM_001039141]	-1.20
TUBA3D*	Homo sapiens tubulin, alpha 3d (TUBA3D), mRNA [NM_080386]	-1.20
TUBB2B*	Homo sapiens tubulin, beta 2B (TUBB2B), mRNA [NM_178012]	-1.07
TUBB6*	Homo sapiens tubulin, beta 6 (TUBB6), mRNA [NM_032525]	-1.21
UTRN*	Homo sapiens utrophin (UTRN), mRNA [NM_007124]	-1.01

Table S7. List of shared genes whose expressions were upregulated in cells exposed to both CuO-NPs and released Cu ions. Fold-change is represented by logarithmic ratio (log_2 ratio) to expression level in control.

Gene name	Description	Fold-change (log_2 ratio)	
		CuO-NPs	Cu ions
MT1F	Homo sapiens metallothionein 1F (MT1F), mRNA [NM_005949]	4.80	4.59
NR4A1	Homo sapiens nuclear receptor subfamily 4, group A, member 1 (NR4A1), transcript variant 1, mRNA [NM_002135]	5.28	2.71
LOC100129113	Homo sapiens cDNA FLJ37158 fis, clone BRACE2026293. [AK094477]	2.71	2.31
DHRS2	Homo sapiens dehydrogenase/reductase (SDR family) member 2 (DHRS2), transcript variant 1, mRNA [NM_182908]	2.45	2.24
CSTA	Homo sapiens cystatin A (stefin A) (CSTA), mRNA [NM_005213]	2.15	2.12
VCX3A	Homo sapiens variable charge, X-linked 3A (VCX3A), mRNA [NM_016379]	5.29	2.11
MT1G	Homo sapiens metallothionein 1G (MT1G), mRNA [NM_005950]	2.31	2.10
NUPR1	Homo sapiens nuclear protein 1 (NUPR1), transcript variant 1, mRNA [NM_001042483]	2.40	2.10
MT2A	Homo sapiens metallothioncin 2A (MT2A), mRNA [NM_005953]	2.24	1.98
CDK5R2	Homo sapiens cyclin-dependent kinase 5, regulatory subunit 2 (p39) (CDK5R2), mRNA [NM_003936]	2.06	1.96
MT1E	Homo sapiens unknown mRNA. [AF495759]	2.16	1.95
HTRA3	Homo sapiens HtrA serine peptidase 3 (HTRA3), mRNA [NM_053044]	2.51	1.93
LOC133874	Homo sapiens hypothetical gene LOC133874 (LOC133874), mRNA [NM_001102609]	1.92	1.84
S100P	Homo sapiens S100 calcium binding protein P (S100P), mRNA [NM_005980]	2.15	1.84
MT1A	Homo sapiens metallothionein 1A (MT1A), mRNA [NM_005946]	2.19	1.75
MT1X	Homo sapiens metallothionein 1X (MT1X), mRNA [NM_005952]	1.98	1.71
SPANXD	Homo sapiens SPANX family, member D (SPANXD), mRNA [NM_032417]	2.54	1.68
GABARAPL1	Homo sapiens GABA(A) receptor-associated protein like 1 (GABARAPL1), mRNA [NM_031412]	4.44	1.62
MT1B	Homo sapiens metallothionein 1B (MT1B), mRNA [NM_005947]	2.24	1.60
INSIG1	Homo sapiens insulin induced gene 1 (INSIG1), transcript variant 2, mRNA [NM_198336]	2.42	1.58
MT1H	Homo sapiens metallothioncin 1H (MT1H), mRNA [NM_005951]	1.98	1.57
SPANXA1	Homo sapiens sperm protein associated with the nucleus, X-linked, family member A1 (SPANXA1), mRNA [NM_013453]	2.18	1.55
MT1L	Homo sapiens metallothionein 1L (gene/pseudogene) (MT1L), non-coding RNA [NR_001447]	1.79	1.52
BEX2	Homo sapiens brain expressed X-linked 2 (BEX2), mRNA [NM_032621]	3.29	1.49
SPANXB2	Homo sapiens SPANX family, member B2 (SPANXB2), mRNA [NM_145664]	2.20	1.48
SNX8	Homo sapiens sorting nexin 8 (SNX8), mRNA [NM_013321]	1.80	1.45
KIAA0430	Homo sapiens KIAA0430 (KIAA0430), mRNA [NM_014647]	1.47	1.44
IGF2	Homo sapiens insulin-like growth factor 2 (somatomedin A) (IGF2), transcript variant 1, mRNA [NM_000612]	1.36	1.47
CLCN6	Homo sapiens chloride channel 6 (CLCN6), transcript variant ClC-6a, mRNA [NM_001286]	1.73	1.32
ASNS	Homo sapiens asparagine synthetase, mRNA (cDNA clone IMAGE:5266877), **** WARNING: chimeric clone ****. [BC030024]	1.58	1.32
PNPLA8	Homo sapiens patatin-like phospholipase domain containing 8 (PNPLA8), mRNA [NM_015723]	2.06	1.27
TAF8	Homo sapiens TAF8 RNA polymerase II, TATA box binding protein (TBP)-associated factor, 43kDa, mRNA (cDNA clone IMAGE:5166848), with apparent retained intron. [BC033728]	1.29	1.24
TRIB3	Homo sapiens tribbles homolog 3 (Drosophila) (TRIB3), mRNA [NM_021158]	1.57	1.20
SEC61A2	Homo sapiens Sec61 alpha 2 subunit (S. cerevisiae) (SEC61A2), transcript variant 1, mRNA [NM_018144]	1.72	1.15
OR5L2	Homo sapiens olfactory receptor, family 5, subfamily L, member 2 (OR5L2), mRNA [NM_001004739]	1.36	1.14

FXC1	Homo sapiens fracture callus 1 homolog (rat) (FXC1), nuclear gene encoding mitochondrial protein, mRNA [NM_012192]	1.13	1.14
BNIP3L	Homo sapiens BCL2/adenovirus E1B 19kDa interacting protein 3-like (BNIP3L), mRNA [NM_004331]	2.17	1.11
PPP1R3B	Homo sapiens protein phosphatase 1, regulatory (inhibitor) subunit 3B (PPP1R3B), mRNA [NM_024607]	1.14	1.10
SIRT6	Homo sapiens sirtuin (silent mating type information regulation 2 homolog) 6 (S. cerevisiae) (SIRT6), mRNA [NM_016539]	1.68	1.10
CYB5R2	Homo sapiens cytochrome b5 reductase 2 (CYB5R2), mRNA [NM_016229]	1.08	1.11
GDF15	Homo sapiens growth differentiation factor 15 (GDF15), mRNA [NM_004864]	1.08	1.95
CTSL2	Homo sapiens cathepsin L2 (CTSL2), mRNA [NM_001333]	1.44	1.07
SOD2	Homo sapiens superoxide dismutase 2, mitochondrial (SOD2), nuclear gene encoding mitochondrial protein, transcript variant 2, mRNA [NM_001024465]	1.28	1.07
C1S	Homo sapiens complement component 1, s subcomponent (C1S), transcript variant 1, mRNA [NM_001734]	1.06	1.21
MSI2	Homo sapiens musashi homolog 2 (Drosophila) (MSI2), transcript variant 2, mRNA [NM_170721]	1.52	1.06
SREBF2	Homo sapiens sterol regulatory element binding transcription factor 2 (SREBF2), mRNA [NM_004599]	1.32	1.06
LARP4	Homo sapiens La ribonucleoprotein domain family, member 4 (LARP4), transcript variant 2, mRNA [NM_199188]	1.76	1.05
MVD	Homo sapiens mevalonate (diphospho) decarboxylase (MVD), mRNA [NM_002461]	1.04	1.61
SEC14L1	Homo sapiens SEC14-like 1 (S. cerevisiae) (SEC14L1), transcript variant 1, mRNA [NM_003003]	1.72	1.03
NFATC1	Homo sapiens nuclear factor of activated T-cells, cytoplasmic, calcineurin-dependent 1 (NFATC1), transcript variant 1, mRNA [NM_172390]	1.83	1.03
TBC1D15	Homo sapiens TBC1 domain family, member 15 (TBC1D15), mRNA [NM_022771]	1.98	1.02
SAT1	Homo sapiens spermidine/spermine N1-acetyltransferase 1 (SAT1), mRNA [NM_002970]	1.53	1.02
C10orf35	Homo sapiens chromosome 10 open reading frame 35 (C10orf35), mRNA [NM_145306]	1.37	1.02
RNF12	Homo sapiens ring finger protein 12 (RNF12), transcript variant 1, mRNA [NM_016120]	1.68	1.01

Table S8. List of shared genes whose expressions were downregulated in cells exposed to both CuO-NPs and released Cu ions. Fold-change is represented by logarithmic ratio (log_2 ratio) to expression level in control.

Gene name	Description	Fold-change (log_2 ratio)	
		CuO-NPs	Cu ions
FAM83D	Homo sapiens family with sequence similarity 83, member D (FAM83D), mRNA [NM_030919]	-2.40	-2.25
HMGB2	Homo sapiens high-mobility group box 2 (HMGB2), transcript variant 1, mRNA [NM_002129]	-2.06	-1.83
IGFBP3	Homo sapiens insulin-like growth factor binding protein 3 (IGFBP3), transcript variant 1, mRNA [NM_001013398]	-2.40	-1.81
CENPA	Homo sapiens centromere protein A (CENPA), transcript variant 1, mRNA [NM_001809]	-1.80	-2.04
TRIM59	Homo sapiens tripartite motif-containing 59 (TRIM59), mRNA [NM_173084]	-1.86	-1.59
KIF20A	Homo sapiens kinesin family member 20A (KIF20A), mRNA [NM_005733]	-2.05	-1.53
MYBL1	Homo sapiens v-myb myeloblastosis viral oncogene homolog (avian)-like 1 (MYBL1), mRNA [NM_001080416]	-1.84	-1.48
CKAP2	Homo sapiens cytoskeleton associated protein 2 (CKAP2), transcript variant 1, mRNA [NM_018204]	-1.76	-1.44
LOC338620	Homo sapiens hypothetical protein LOC338620, mRNA (cDNA clone IMAGE:6023208), partial cds. [BC043009]	-2.01	-1.42
TOP2A	Homo sapiens topoisomerase (DNA) II alpha 170kDa (TOP2A), mRNA [NM_001067]	-2.00	-1.41
CCDC80	Homo sapiens coiled-coil domain containing 80 (CCDC80), transcript variant 1, mRNA [NM_199511]	-1.40	-1.41
BARD1	Homo sapiens BRCA1 associated RING domain 1 (BARD1), mRNA [NM_000465]	-1.35	-1.55
CCNB1	Homo sapiens cyclin B1 (CCNB1), mRNA [NM_031966]	-1.74	-1.33
G0S2	Homo sapiens G0/G1switch 2 (G0S2), mRNA [NM_015714]	-1.33	-1.56
NFE2L3	Homo sapiens nuclear factor (erythroid-derived 2)-like 3 (NFE2L3), mRNA [NM_004289]	-1.99	-1.32
ZNF185	Homo sapiens zinc finger protein 185 (LIM domain) (ZNF185), mRNA [NM_007150]	-1.28	-1.77
ALPK2	Homo sapiens alpha-kinase 2 (ALPK2), mRNA [NM_052947]	-1.58	-1.28
PABPC3	Homo sapiens poly(A) binding protein, cytoplasmic 3 (PABPC3), mRNA [NM_030979]	-1.71	-1.26
SLC27A2	Homo sapiens solute carrier family 27 (fatty acid transporter), member 2 (SLC27A2), mRNA [NM_003645]	-1.26	-1.57
HN1	Homo sapiens hematological and neurological expressed 1 (HN1), transcript variant 3, mRNA [NM_001002033]	-1.25	-1.32
C15orf23	Homo sapiens chromosome 15 open reading frame 23 (C15orf23), transcript variant 2, mRNA [NM_001142761]	-1.63	-1.24
CDC20	Homo sapiens cell division cycle 20 homolog (S. cerevisiae) (CDC20), mRNA [NM_001255]	-1.23	-1.42
EFEMP1	Homo sapiens EGF-containing fibulin-like extracellular matrix protein 1 (EFEMP1), transcript variant 1, mRNA [NM_004105]	-1.78	-1.22
RACGAP1	Homo sapiens Rac GTPase activating protein 1 (RACGAP1), transcript variant 1, mRNA [NM_013277]	-1.56	-1.22
KIF23	Homo sapiens kinesin family member 23 (KIF23), transcript variant 1, mRNA [NM_138555]	-1.56	-1.21
TUBA3D	Homo sapiens tubulin, alpha 3d (TUBA3D), mRNA [NM_080386]	-1.20	-1.32
LOC100128974	PREDICTED: Homo sapiens misc_RNA (LOC100128974), miscRNA [XR_037045]	-1.31	-1.19
LMNB2	Homo sapiens lamin B2 (LMNB2), mRNA [NM_032737]	-1.71	-1.19
PLAGL1	Homo sapiens pleiomorphic adenoma gene-like 1 (PLAGL1), transcript variant 2, mRNA [NM_006718]	-1.18	-1.50
CCNA2	Homo sapiens cyclin A2 (CCNA2), mRNA [NM_001237]	-1.39	-1.18
PRSS23	Homo sapiens protease, serine, 23 (PRSS23), mRNA [NM_007173]	-1.80	-1.17
TPX2	Homo sapiens TPX2, microtubule-associated, homolog (Xenopus laevis) (TPX2), mRNA [NM_012112]	-1.25	-1.17
PIF1	Homo sapiens PIF1 5'-to-3' DNA helicase homolog (S. cerevisiae) (PIF1), mRNA [NM_025049]	-1.65	-1.16
CDC2	Homo sapiens cell division cycle 2, G1 to S and G2 to M (CDC2), transcript variant 1, mRNA [NM_001786]	-1.41	-1.16
RRM2	Homo sapiens ribonucleotide reductase M2 polypeptide (RRM2), mRNA [NM_001034]	-1.38	-1.15
SFRP1	Homo sapiens secreted frizzled-related protein 1 (SFRP1), mRNA [NM_003012]	-1.14	-1.16
TMEM171	Homo sapiens transmembrane protein 171 (TMEM171), mRNA [NM_173490]	-1.15	-1.14
GPSM2	Homo sapiens G-protein signaling modulator 2 (AGS3-like, C. elegans) (GPSM2), mRNA [NM_013296]	-1.19	-1.14
TRIM14	Homo sapiens tripartite motif-containing 14 (TRIM14), transcript variant 1, mRNA [NM_014788]	-1.87	-1.13
TRAM1	Homo sapiens translocation associated membrane protein 1 (TRAM1), mRNA [NM_014294]	-1.11	-1.40
LOC389842	PREDICTED: Homo sapiens similar to RanBP1 (LOC389842), mRNA [XM_372200]	-1.44	-1.11
TPM1	Homo sapiens tropomyosin 1 (alpha) (TPM1), transcript variant 5, mRNA [NM_000366]	-1.09	-1.55
HYLS1	Homo sapiens hydrolethalus syndrome 1 (HYLS1), transcript variant 1, mRNA [NM_145014]	-1.25	-1.09
TMSB4X	Homo sapiens thymosin beta 4, X-linked (TMSB4X), mRNA [NM_021109]	-1.13	-1.09
IRS1	Homo sapiens insulin receptor substrate 1 (IRS1), mRNA [NM_005544]	-2.21	-1.08
ABCB10	Homo sapiens ATP-binding cassette, sub-family B (MDR/TAP), member 10 (ABCB10), nuclear gene encoding mitochondrial protein, mRNA [NM_012089]	-1.70	-1.07
KIF18B	Homo sapiens hypothetical protein LOC146909, mRNA (cDNA clone IMAGE:4418755), partial cds. [BC048263]	-2.07	-1.07
LOC100132658	PREDICTED: Homo sapiens misc_RNA (LOC100132658), miscRNA [XR_038952]	-1.15	-1.07
FBXO5	Homo sapiens F-box protein 5 (FBXO5), transcript variant 1, mRNA [NM_012177]	-1.17	-1.06
TGFB2	Homo sapiens transforming growth factor, beta 2 (TGFB2), transcript variant 1, mRNA [NM_001135599]	-2.11	-1.05
CDCA3	Homo sapiens cell division cycle associated 3 (CDCA3), mRNA [NM_031299]	-1.34	-1.04
AREG	Homo sapiens amphiregulin (AREG), mRNA [NM_001657]	-1.50	-1.02
ZFP36L1	Homo sapiens zinc finger protein 36, C3H type-like 1 (ZFP36L1), mRNA [NM_004926]	-1.45	-1.02
DLGAP5	Homo sapiens discs, large (Drosophila) homolog-associated protein 5 (DLGAP5), mRNA [NM_014750]	-1.34	-1.01
BCAR3	Homo sapiens breast cancer anti-estrogen resistance 3 (BCAR3), mRNA [NM_003567]	-1.10	-1.00

Table S9. Shared downregulated genes by CuO-NPs and released Cu ions, which fall into the categories of "mitosis", chromosome segregation", and "cell cycle".

GO category	Gene name	Description
mitosis	CCNA2	Homo sapiens cyclin A2 (CCNA2), mRNA [NM_001237]
	CCNB1	Homo sapiens cyclin B1 (CCNB1), mRNA [NM_031966]
	CDC2	Homo sapiens cell division cycle 2, G1 to S and G2 to M (CDC2), transcript variant 1, mRNA [NM_001786]
	GPSM2	Homo sapiens G-protein signaling modulator 2 (AGS3-like, C. elegans) (GPSM2), mRNA [NM_013296]
	KIF18B	Homo sapiens hypothetical protein LOC146909, mRNA (cDNA clone IMAGE:4418755), partial cds. [BC048263]
	KIF20A	Homo sapiens kinesin family member 20A (KIF20A), mRNA [NM_005733]
	KIF23	Homo sapiens kinesin family member 20A (KIF20A), mRNA [NM_005733]
	TOP2A	Homo sapiens topoisomerase (DNA) II alpha 170kDa (TOP2A), mRNA [NM_001067]
	TPX2	Homo sapiens TPX2, microtubule-associated, homolog (Xenopus laevis) (TPX2), mRNA [NM_012112]
	TUBA3D	Homo sapiens tubulin, alpha 3d (TUBA3D), mRNA [NM_080386]
	ZFP36L1	Homo sapiens zinc finger protein 36, C3H type-like 1 (ZFP36L1), mRNA [NM_004926]
chromosome segregation	KIF18B	Homo sapiens hypothetical protein LOC146909, mRNA (cDNA clone IMAGE:4418755), partial cds. [BC048263]
	KIF20A	Homo sapiens kinesin family member 20A (KIF20A), mRNA [NM_005733]
	KIF23	Homo sapiens kinesin family member 20A (KIF20A), mRNA [NM_005733]
	TOP2A	Homo sapiens topoisomerase (DNA) II alpha 170kDa (TOP2A), mRNA [NM_001067]
	TPX2	Homo sapiens TPX2, microtubule-associated, homolog (Xenopus laevis) (TPX2), mRNA [NM_012112]
	TUBA3D	Homo sapiens tubulin, alpha 3d (TUBA3D), mRNA [NM_080386]
cell cycle	CCNA2	Homo sapiens cyclin A2 (CCNA2), mRNA [NM_001237]
	CCNB1	Homo sapiens cyclin B1 (CCNB1), mRNA [NM_031966]
	CDC2	Homo sapiens cell division cycle 2, G1 to S and G2 to M (CDC2), transcript variant 1, mRNA [NM_001786]
	CDC20	Homo sapiens cell division cycle 20 homolog (S. cerevisiae) (CDC20), mRNA [NM_001255]
	GPSM2	Homo sapiens G-protein signaling modulator 2 (AGS3-like, C. elegans) (GPSM2), mRNA [NM_013296]
	KIF18B	Homo sapiens hypothetical protein LOC146909, mRNA (cDNA clone IMAGE:4418755), partial cds. [BC048263]
	KIF20A	Homo sapiens kinesin family member 20A (KIF20A), mRNA [NM_005733]
	KIF23	Homo sapiens kinesin family member 20A (KIF20A), mRNA [NM_005733]
	MYBL1	Homo sapiens v-myb myeloblastosis viral oncogene homolog (avian)-like 1 (MYBL1), mRNA [NM_001080416]
	TOP2A	Homo sapiens topoisomerase (DNA) II alpha 170kDa (TOP2A), mRNA [NM_001067]
	TPX2	Homo sapiens TPX2, microtubule-associated, homolog (Xenopus laevis) (TPX2), mRNA [NM_012112]
	TRIM14	Homo sapiens tripartite motif-containing 14 (TRIM14), transcript variant 1, mRNA [NM_014788]
	TRIM59	Homo sapiens tripartite motif-containing 59 (TRIM59), mRNA [NM_173084]
	TUBA3D	Homo sapiens tubulin, alpha 3d (TUBA3D), mRNA [NM_080386]
	ZFP36L1	Homo sapiens zinc finger protein 36, C3H type-like 1 (ZFP36L1), mRNA [NM_004926]

Table S10. Primer sequences for qPCR

Gene Name	Forward sequence (5'→3')	Reverse sequence (5'→3')
GADD45A	ctgaacggtgatggcatctg	ccccttggcatcagtttctg
GADD45B	taccgttggtttccgcaact	gccagagagcccaaaacctt
GADD45G	gtgctgagctctggctgtca	gctgtgctttccggaactgt
PCNA	ggtgttggaggcactcaagg	ccaaagagacgtgggacgag
CDC2	ttcagagctttgggcactcc	gggatgctaggcttcctggt
CCNB1	actgcaggccaaaatgccta	aggttctggctctggcactg
CDKN1A	tcctctagctgtgggggtga	aaggtcgctggacgatttga
FOS	cctcgtactccaaccgcatc	tgggtaggagcacggtcact
FOSB	caagaggtacagcggcatcc	caacgtcccgttccaacaat
ATF3	tgggtccagaagacctgcat	aaaccctggtgatgccacag
JDP2	tgaaggaggcaggacagagg	tcatggcttttcctggctgt
ATR	gctctggtccaagggtgatg	accctcaggtggggtttcat
TP53	cgtcccaagcaatggatgat	tggcattctgggagcttcat
NR4A1	gcaccttcatggacggctac	ctgaggagcatggctggact
NR4A2	tgtaccaaatgcccctgtcc	gagtgcggcatcatctcctc
NR4A3	agccttcctgcgtgtaccaa	aatggatggctgctgatgct
AURKA	tcagcgggtcttgtgtcctt	aaccggcttgtgactggaga
AURKB	ccccatctgcacttgtcctc	tgtgaagtgccgcgttaaga
TPX2	ccccctcggatttcatcaat	ttggccttctcctcaaacca

SCIENTIFIC REPORTS

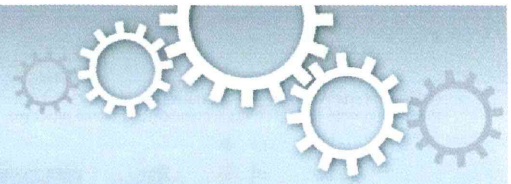

OPEN

SUBJECT AREAS:
MATERIALS
NANOBIOTECHNOLOGY
NANOPARTICLES
BIOMATERIALS

Received
12 March 2012

Accepted
30 April 2012

Published
14 May 2012

Correspondence and requests for materials should be addressed to M.S.X. (msxu@zju.edu.cn) or N.H. (HANAGATA.Nobutaka@nims.go.jp)

Formation of Nano-Bio-Complex as Nanomaterials Dispersed in a Biological Solution for Understanding Nanobiological Interactions

Mingsheng Xu[1], Jie Li[2], Hideo Iwai[3], Qingsong Mei[4], Daisuke Fujita[5], Huanxing Su[6], Hongzheng Chen[1] & Nobutaka Hanagata[2]

[1]State Key Laboratory of Silicon Materials, MOE Key Laboratory of Macromolecule Synthesis and Functionalization & Department of Polymer Science and Engineering, Zhejiang University, Hangzhou 310027, P. R. China, [2]Nanotechnology Innovation Station, National Institute for Materials Science, 1-2-1 Sengen, Tsukuba, Ibaraki 305-0047, Japan, [3]Research Network and Facility Services Division, Materials Analysis Station, National Institute for Materials Science, 1-2-1 Sengen, Tsukuba, Ibaraki 305-0047, Japan, [4]Department of Materials Engineering, School of Powder and Mechanical Engineering, Wuhan University, Wuhan 430072, China, [5]Advanced Key Technologies Research Division, Nano Characterization Unit, National Institute for Materials Science, 1-2-1 Sengen, Tsukuba, Ibaraki 305-0047, Japan, [6]State Key Laboratory of Quality Research in Chinese Medicine and Institute of Chinese Medical Sciences, University of Macau, Macao SAR, China.

Information on how cells interface with nanomaterials in biological environments has important implications for the practice of nanomedicine and safety consideration of nanomaterials. However, our current understanding of nanobiological interactions is still very limited. Here, we report the direct observation of nanomaterial bio-complex formation (other than protein corona) from nanomaterials dispersed in biologically relevant solutions. We observed highly selective binding of the components of cell culture medium and phosphate buffered saline to ZnO and CuO nanoparticles, independent of protein molecules. Our discoveries may provide new insights into the understanding of how cells interact with nanomaterials.

Nanotechnology has held great promise for revolutionizing biomedicine. Nanomaterials (NMs) are widely being under investigation for bioimaging[1], killing tumors[2], delivering drugs/genes[3,4]. The response of biological systems to NMs depends primarily on the surface properties of NMs in a biological environment[5,6]. For example, there is increasing evidence of rapid formation of protein coronas, as NMs within biological environments acquire a coating of protein molecules[7–11], and thus there is some consensus that cellular responses to materials in a biological medium reflect the adsorbed biomolecule layer, rather than the material itself. The concept of the nanoparticle (NP) protein corona is important towards understanding the dynamic surface properties of NMs in biological environments. Unfortunately, the interface issues between NMs and biological systems are too complicated and it is still not very clear how the spontaneous formation of a protein corona influences the materials' interactions with biological systems and contributes to biological outcomes of materials. On the other hand, the increasing use of NMs in industrial and consumer products has aroused global concern regarding their potential impact on the environment and human health. Although a number of studies on the effects of NMs in *in vitro* and *in vivo* systems have been published[12–17], there are still many challenges and issues[12–14] encountered at the interface between NMs and biological systems when assessing the toxicity of NMs. As demonstrated here the state of NMs in biological environments is more complicated than previously thought, requiring a more holistic understanding of what happen as NMs are dispersed in the local biological environments and what cells interface in such an environment. Not only does the biological interface of NMs need to be understood and controlled, but also NMs should be treated as biological entities rather than inorganic ones[6]. The understanding of nano-bio interactions could help in promoting applications of NMs in the biomedical fields and reducing/preventing possible adverse effects to the biological systems caused by NMs.

Here, we present the first report in nanobiological field, to our knowledge, describing nanomaterial (NM) bio-complexes or ion corona formed from the binding of NMs with non-protein components in a biological

environment. We observed highly selective binding of the components of cell culture medium and phosphate buffered saline (PBS) to ZnO and CuO nanoparticles (NPs), independent of protein molecules. Our findings would be helpful to understand nano-bio-interactions, allowing to effectively modifying NM surfaces for specifically biomedical applications.

Results

We observed that ZnO and CuO NPs can bind various constituents from biological environments to form NM bio-complexes or ion corona. The reason that we call the formed clusters as bio-complex is that the NMs are used for biological applications, though it may not involve biological molecules. Figure 1 presents the transmission electron microscopy (TEM) elemental maps of ZnO NPs dispersed in high-glucose Dulbecco's modified Eagle's medium (DMEM) without fetal bovine serum (FBS). In addition to aggregation/agglomeration of the NPs[15], the elemental maps clearly illustrate the binding of ZnO NPs to components of the medium to form NP bio-complexes. We detected Ca, Na, K, P, and Cl originating from the medium (components of DMEM are listed in Supplementary Information). For comparison, we examined the effects of FBS and PBS on the formation of NP bio-complexes. High-resolution TEM images (Fig. 2a and Supplementary Fig. S1) show that in medium supplemented with 10% FBS the crystalline ZnO NPs (see Supplementary Fig. S1) are surrounded by compounds, indicating NP bio-complex formation. Furthermore, we found that these bio-complexes also formed when the ZnO NPs were dispersed in PBS, either with (Supplementary Figs. S2–3) or without FBS (Fig. 2b). We confirmed that the observed highly ordered crystalline structures are ZnO NPs because no crystalline structures were detected in the control suspensions where no ZnO NP was dispersed in medium or PBS (Supplementary Figs. S4–7, S10). These results clearly suggest that the formation of NP bio-complexes in biological environments (medium and PBS) occurs independently of serum proteins. The formation of protein coronas and the adsorption of different proteins onto NPs affect the uptake and transport of NPs in biological systems[7–11]. We believe that the biological behavior of NPs could be similarly modified by the formation of NP bio-complexes.

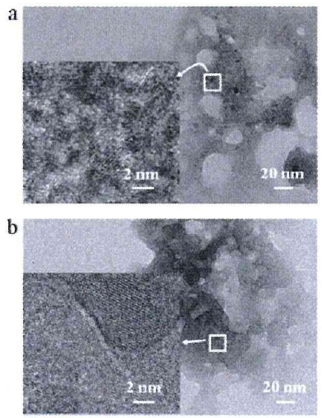

Figure 2 | Surrounded nanoparticles. (a) TEM image of ZnO NPs dispersed in medium supplemented with fetal bovine serum; (b) TEM image of ZnO NPs dispersed in PBS without fetal bovine serum. The inset high-resolution TEM images clearly suggest that ZnO NP (dark-colored) bio-complexes were formed.

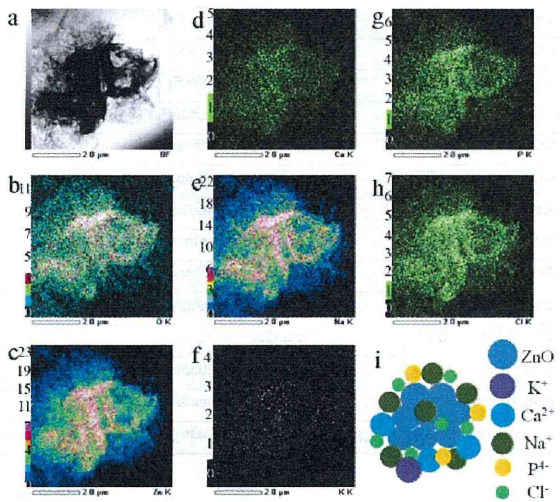

Figure 1 | Formation of ZnO nanoparticle bio-complexes in medium without fetal bovine serum. (a) TEM image showing where the elemental maps were obtained; (b) TEM/EDS O-K map; (c) TEM/EDS Zn-K map; (d) TEM/EDS Ca-K map; (e) TEM/EDS Na-K map; (f) TEM/EDS K-K map; (g) TEM/EDS P-K map; (h) TEM/EDS Cl-K map; (i) A simple model of ZnO bio-complexes.

Figure 3 displays the TEM elemental maps of CuO NPs dispersed in the DMEM supplemented with 10% FBS. By comparing the relative contrast of the maps in Fig. 1 and Supplementary Fig. S1 to that in Fig. 3, we determined that the ZnO and CuO NPs exhibited different binding affinities for the various components of the medium. As plotted in Fig. 4a, in the case of the NPs dispersed in DMEM with FBS, the ZnO NPs bound more Na than Ca and more P than Cl, whereas the CuO NPs bound more Ca than Na and more P than Cl. This selective adsorption may be similar to that seen in the formation of protein coronas, which is reported to be influenced by particle chemistry[9]. Furthermore, FBS has effort on the binding behavior of ions as we can see from Fig. 4a that the ZnO NPs which were dispersed in DMEM with FBS bound more Cl than P, indicating biological environment may also influence the binding process. In addition, as highlighted in Fig. 4b, we observed NP-like clusters that apparently do not contain CuO or ZnO NPs; we believe they arose from components of the cell culture medium. Hence, the bio-complexes and the NP-like clusters can influence size distribution of particles in the biological systems, suggesting caution should be taken as addressing size effects of NMs on biological behaviors.

To confirm the selective binding of ions by the NPs, we used X-ray photoelectron spectroscopy (XPS) to investigate the ensemble of ZnO NPs and CuO NPs after dispersed in the DMEM or DMEM with FBS. Table 1 summarizes the atomic concentrations of the main elements bound by the NPs. In the case of the NPs ensemble dispersed in the DMEM with FBS, the orders of estimated atomic concentration of elements bound by ZnO NPs and by CuO NPs are Na1s (2.8%) > P2s (0.8%) > Ca2p (0.7%) > Cl2p (0.6%) and Na1s (2.6%) > Ca2p (1.8%) > P2s (1.0%) > Cl2p (0.5%), respectively. From Table 1, we also found that FBS affected the ion binding as compared the ZnO NPs dispersed in DMEM to that dispersed in DMEM with FBS. These XPS results are in good agreement with the TEM observation on the individual NPs.

Although we did not detect obvious signal of N, a main component of protein, by TEM, we detected it by XPS due to much lower energy of the used X-ray than the electron beam used for TEM observation. The N1s atomic concentration of the ZnO NPs dispersed in DMEM with FBS is much higher than that of the ZnO NPs dispersed in

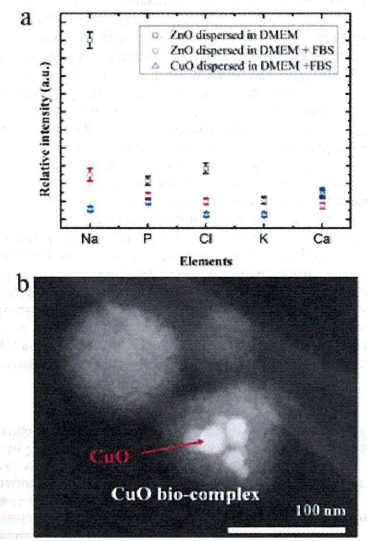

Figure 4 | Selective binding of ions by ZnO and CuO NPs. (a) Scattering plot of bound elements by ZnO and CuO NPs from the DMEM or DMEM with FBS, comparatively showing different binding affinities for the various components of the DMEM or DMEM with FBS by the NPs. The standard deviation error bars were based on the results obtained at three different sample regions; (b) Dark-field TEM image of CuO NPs suspension (25 μg/mL) in medium with FBS, showing nanoparticle-like clusters that apparently do not contain CuO NPs.

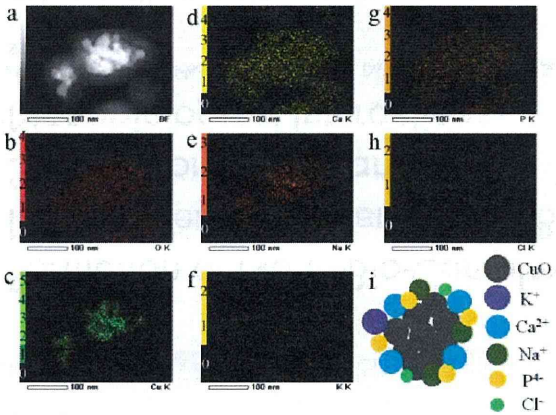

Figure 3 | Formation of CuO nanoparticle bio-complexes in medium with fetal bovine serum. (a) Dark-field TEM image showing where the elemental maps were obtained; (b) TEM/EDS O-K map; (c) TEM/EDS Zn-K map; (d) TEM/EDS Ca-K map; (e) TEM/EDS Na-K map; (f) TEM/EDS K-K map; (g) TEM/EDS P-K map; (h) TEM/EDS Cl-K map; (i) A simple model of CuO bio-complexes.

Table 1 | Atomic concentration (at%) of main elements estimated on the basis of the wide XPS spectra of ZnO and CuO NPs dispersed in DMEM or DMEM with FBS

	N1s	O1s	Na1s	P2s	Cl2p	K2p	Ca2p	Zn2p3/2	Cu2p3/2
#1	2.4	45.6	9.4	1.7	0.7	0.2	2.2	19.5	
#2	9.8	28.0	2.8	0.8	0.5	0.1	0.7	5.4	
#3	10.3	30.1	2.6	1.0	0.5	0.1	1.8		5.9

#1, #2 and #3 represent ZnO NPs dispersed in DMEM, ZnO NPs dispersed in DMEM with FBS and CuO NPs dispersed in DMEM with FBS, respectively.

DMEM. Furthermore, the binding energy of one of the fit peaks of N1s spectra shifted to 399.76 eV (Fig. 5b) or 399.70 eV (Fig. 5c) from 399.41 eV of the pristine FBS (Supplementary Fig. S15b and Table S1). The shift suggests protein molecules in the FBS may bind to the NPs, forming protein corona.

As shown in Figs. 5d–f and Supplementary Figs. S15c–d, we detected different shifts, toward a lower binding energy in contrast to a higher binding energy of the N1s (Figs. 5b–c), of the Na1s and Cl2p binding energies as they contacted with ZnO NPs in DMEM or DMEM with FBS from the pristine DMEM and FBS. The different shift may indicate various interactions between the ions and ZnO NPs in the different solution environments. The various interactions reflect the change of zeta potential of the NPs dispersed in the different solvents as shown in Fig. 6. For instance, the zeta potential of ZnO NPs changed from a negative value in de-ionized water (DI water) to a positive value as dispersed in DMEM or DMEM with FBS. The change of zeta potential of ZnO and CuO NPs is believed to be due to the binding of ions from the solvents, which is consistent with the selective binding of ions by the ZnO and CuO NPs.

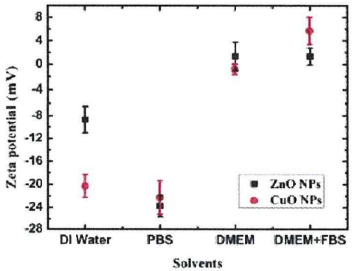

Figure 6 | Various zeta potentials of ZnO and CuO NPs dispersed in different solvents. The change of zeta potential suggests ZnO and CuO NPs bound various ions in the solutions. The error bars represent standard deviation based on three independent measurements of each sample.

Discussion

We have shown that ZnO and CuO NPs formed bio-complex or ion corona by selectively absorbing components or ions from the DMEM, DMEM supplemented with FBS, and PBS. The formation of bio-complexes is not associated with serum proteins. The discovery of bio-complex formation offers new insights for interpreting the observation that the uptake of negatively charged NPs by cells is greater than that of non-functionalized NPs[18,19]. This phenomenon is contradictory to the well-established concept that positively charged NPs have high affinity to the negatively charged cell membrane, and the unfavorable interaction was partially attributed to the formation of NP protein corona[19]. For instance, it has recently been

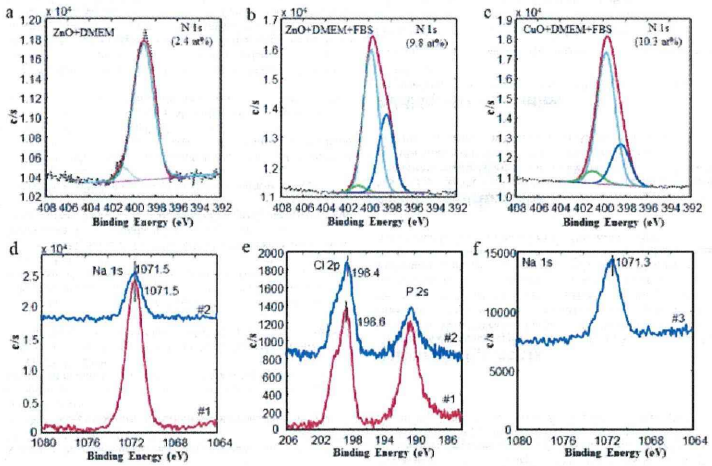

Figure 5 | XPS characterization of selectively bound ions by ZnO and CuO NPs. (a) N1s curve fit of ZnO NPs dispersed in DMEM; (b) N1s curve fit of ZnO NPs dispersed in DMEM with FBS; (c) N1s curve fit of CuO NPs dispersed in DMEM with FBS; (d) Na1s spectra of ZnO NPs dispersed in DMEM (#1) and in DMEM with FBS (#2); (e) Cl2p spectra of ZnO NPs dispersed in DMEM (#1) and in DMEM with FBS (#2); (f) Na1s spectra of CuO NPs dispersed in DMEM with FBS (#3). Compared to the binding energies of the elements of the pristine DMEM and FBS, the binding energy positions in the spectra were shifted.

shown that negatively charged Au NPs are more toxic than positively charged and neutral Au NP counterparts, due to the interaction of the outer Au NP components with cellular components[20]. The interaction of the negatively charged Au NPs with cellular components could in turn influence the mitochondrial membrane potential by releasing positively charged calcium ions from the matrix into the cytosol[20]. Thus, previous work related to the effects of surface charge and surface modification on cell-specific responses and cytotoxicity[21–23] may need to be re-evaluated. That is, the surface may not the one as expected from the intended surface modification. Our finding that NP bio-complexes form in biological environments could be used to help design the NP surfaces for effective drug, DNA and siRAN delivery systems and more accurate nanotoxicity studies.

We did not detect signals from key components of serum proteins, such as N, due to the high energy of the electron beam used in the TEM technique. However, we did observe the disappearance of certain matters during the TEM observation because biomolecules can be easily damaged by high energy beam, which may have been the serum proteins. Previously, Maiorano *et al.* made the assumption that an observed cloud surrounding Au NPs was caused by proteins, based on TEM observations without corresponding elemental maps[24]. Despite this assumption, protein coronas can mediate cellular responses[6] and the toxic effects of NMs[24,25]. We believe that identification of the constituents of NP bio-complexes would significantly improve our understanding of what is selectively acquired by NMs in biological environments; how those acquired constituents influence the reactivity, transport, transformation, bioavailability, and toxicity of NMs; and how the NMs interact with living cells[26,27].

Although there is implication that the binding components from cellular environment had great effects on the toxicity of Au NPs[20], it is currently impossible to describe with certainty all the interactions play at the nano-bio interface in biological environments. The concept of the NP protein corona is important in understanding the dynamic surface properties of NMs in biological fluids. However, even at this moment, it is less clear how the spontaneous formation of a protein corona influences the materials' interactions with biological surfaces and receptors and contributes to biological outcomes of materials. Although it is not surprising that NPs would aggregate in salt rich solutions as this is well known from colloidal theory, the present observation of NMs bio-complexes is certainly new, and such kind of ion corona may be assumed as protein corona if there is no elemental identification[24]. We observed the formation of bio-complexes after naturally drying of the ZnO and CuO NPs immersed in the biological solutions. It remains unclear how dynamically biological environments influence the attaching and detaching of the components from the solution, which is under investigation. Despite challenges to probe events happened at the nano-biointerface, the basic principles of nano-biointerface are being investigated by establishing new imaging techniques, such as TEM and scanning probe microscopy, and biological approaches[5]. The well known colloid chemistry and physics might be considered to be helpful to understand the formation of bio-complexes, however, the behaviors in a biological environment is conceptually different from the well-known colloidal phenomena[6]. By contrast, the methods for protein corona investigation may be extended to explore dynamics of bio-complexes[26,27].

In summary, we have discovered the formation of NM bio-complexes originating from the adsorption of various components in a biological environment onto NMs, independent of proteins. The interaction between NMs and the local environment adds complexity to the challenge of determining the biological outcome of using NMs. Thus, identification of the constituents of these bio-complexes would provide new insights into our understanding of how NMs are modified in biological environments and what cells really see. These results are expected to improve our understanding of the interactions between NMs and live cells. The results of our study are a reminder that our understanding of the nano-bio interactions is still in its infancy.

Methods

Nanoparticles. High-purity ZnO and CuO NPs were obtained from Sigma-Aldrich (Sigma-Aldrich Co., Japan). The primary dimensions and sizes of the oxides were provided in the data sheet, as determined by X-ray diffraction (XRD) and Brunauer–Emmett–Teller (BET) analysis. The average sizes of the ZnO and CuO NPs were 60 nm and 50 nm, respectively, but were not uniform, as previously observed by electron microscopy[16]. In contrast to Au and silica NPs, it is almost impossible to synthesize homogeneous ZnO or CuO NPs with identical shape and size. We characterized the primary size, shape, and composition of the NPs by scanning electron microscopy (SEM) equipped with energy dispersive spectroscopy (EDS) (JSM-7001F, JEOL Inc., Japan) and by X-ray photoelectron spectroscopy (XPS) (PHI Quantera SXM, ULVAC-PHI, Japan)[16]. Note that here we used the averaged primary size as many reports by others[17]. In the regard of varying size of the ZnO and CuO NPs, our observed formation of bio-complex is independent on the size of materials.

Dispersion solvents. DMEM (pH = 7.4) (Invitrogen,) with or without 10% (v/v) FBS (SAFC Bioscience Inc.,) was supplemented with 100 units/mL penicillin and 100 μg/mL streptomycin. The composition of DMEM can be found in the Supplementary Information section. Phosphate buffer saline (PBS) contains $NaHPO_4$, Na_2HPO_4, and NaCl.

Nanoparticle suspension preparation. ZnO and CuO were dispersed in medium with FBS, medium without FBS, PBS, or PBS with FBS. The concentration of the NP suspensions was 25 μg/mL.

TEM characterization. The dark-field TEM images, high-resolution TEM (HRTEM) images, elemental mapping, and EDS were analyzed using a JEM-2100F high-resolution transmission electron microscope (JEOL Inc., Japan) with acceleration voltage of 200 kV. The samples for TEM observation were prepared by immersing TEM mesh into the NP suspension (25 μg/mL) for 24 h at 37°C in the dark with 5% CO_2, the typical cell culture conditions. After naturally drying in air, the TEM mesh was observed.

XPS characterization. PHI Quantera SXM (ULVAC-PHI) with monochromatic Al Kα X-ray (1.5×0.1 mm, 100 W) (pass energy of 55 eV and step of 0.2 eV for narrow spectrum and pass energy of 280 eV and step of 0.5 eV for survey spectrum) was used. Binding energy corrections for the spectra were carried out by using C1s peaks at 285.0 eV. The sample for XPS investigation was prepared by immersing Au substrate into the suspension of NPs in DMEM or DMEM with FBS.

Zeta potential. The surface zeta potentials of the ZnO NPs and CuO NPs were measured by using a laser electrophoresis zeta-potential analyzer (LEZA-600, Otsuka Electronics, Japan). The NPs were dispersed in the solvents with a concentration of 25 μg/mL by sonication for ~60 min to reduce aggregation/agglomeration. The cell unit of the equipment was washed by using the same solvent as that for dispersing NPs prior to measurement. We measured three times for each sample.

1. Chatterjee, D. K., Gnanasammandhan, M. K. & Zhang, Y. Small upconverting fluorescent nanoparticles for biomedical applications. *Small* **6**, 2781–2795 (2010).
2. Kudgus, R. A., Bhattacharya, R. & Mukherjee, P. Cancer nanotechnology: emerging role of gold nanoconjugates. *Anticancer Agents Med. Chem.* **11**, 965–973 (2011).
3. Farokhzad, O. C. & Langer, R. Impact of nanotechnology on drug delivery. *ACS Nano* **3**, 16–20 (2009).
4. Chen, A. M., Taratula, O, Wei, D. G., Yen, H. I., Thomas, T., Thomas, T. J., Minko, T. & He, H. X. Labile catalytic packaging of DNA/siRNA: control of gold nanoparticles "out" of DNA/siRNA complexes. *ACS Nano* **4**, 3679–3688 (2010).
5. Nel, A. E., Mädler, L., Velegol, D., Xia, T., Hoek, E. M. V., Somasundaran, P., Klaessig, F., Castranova, V. & Thompson, M. Understanding biophysicochemical interactions at the nano–bio interface. *Nat. Mater.* **8**, 543–557 (2009).
6. Park, S. & Hamad-Schifferli, K. Nanoscale interfaces to biology. *Curr. Opin. Chem. Biol.* **14**, 616–622 (2010).
7. Keselowsky, B. G., Collard, D. M. & Garcia, A. J. Surface chemistry modulates focal adhesion composition and signaling through changes in integrin binding. *Biomaterials* **25**, 5947–5954 (2004).
8. Cedervall, T., Lynch, I., Lindman, S., Berggard, T., Thulin, E., Nilsson, H., Dawson, K. A. & Linse, S. Understanding the nanoparticle-protein corona using methods to quantify exchange rates and affinities of proteins for nanoparticles. *Proc. Natl. Acad. Sci. U.S.A.* **104**, 2050–2055 (2007).
9. Lunqvist, M., Stigler, J., Elia, G., Lynch, I., Cedervall, T. & Dawson, K. A. Nanoparticle size and surface properties determine the protein corona with possible implications for biological impact. *Proc. Natl. Acad. Sci. U.S.A.* **105**, 14265–14270 (2008).
10. Ehrenberg, M. S., Friedman, A. E., Finkelstein, J. N., Oberdorster, G. & McGrath, J. L. The influence of protein adsorption on nanoparticle association with cultured endothelial cells. *Biomaterials* **30**, 603–610 (2009).

11. Mahmoudi, M., Lynch, I., Ejtehadi, M. R., Monopoli, M. P., Bombelli, F. B. & Laurent, S. Protein-nanoparticle interactions: opportunities and challenges. *Chem. Rev.* **111**, 5610–5637 (2011).
12. Maynard, A. D., Warheit, D. B. & Philbert, M. A. The new toxicology of sophisticated materials: nanotoxicicology and beyond. *Toxicol. Sci.* **120**, S109–S129 (2011).
13. Frug, H. F. & Wick, P. Nanotoxicology: an interdisciplinary challenge. *Angew. Chem. Int. Ed.* **50**, 1260–1278 (2011).
14. Warheit, D. B. Debunking some misconceptions about nanotoxicology. *Nano Lett.* **10**, 4777–4782 (2010).
15. Jiang, J., Oberdörster, G. & Biswas, P. Characterization of size, surface charge, and agglomeration state of nanoparticle dispersions for toxicological studies. *J. Nanopart. Res.* **11**, 77–89 (2009).
16. Xu, M. S., Fujita, D., Kajiwara, S., Minowa, T., Li, X. L., Takemura, T., Iwai, H. & Hanagata, N. Contribution of physicochemical characteristics of nano-oxides to cytotoxicity. *Biomaterials* **31**, 8022–8031 (2010).
17. Xia, T., Kovochich, M., Liong, M., Madler, L., Gilbert, B., Shi, H., Yeh, J. I., Zink, J. I. & Nel, A. E. Comparison of the mechanism of toxicity of zinc oxide and cerium oxide nanoparticles based on dissolution and oxidative stress properties. *ACS Nano* **2**, 2121–2134 (2008).
18. Villanueva, A., Canete, M., Roca, A. G., Calero, M., Veintemillas-Verdaguer, S., Serna, C. J., Morales, M. D. & Miranda, R. The influence of surface functionalization on the enhanced internalization of magnetic nanoparticles in cancer cells. *Nanotechnology* **20**, 115103 (2009).
19. Verma, A. & Stellacci, F. Effect of surface properties on nanoparticle-cell interactions. *Small* **6**, 12–21 (2010).
20. Schaeublin, N. M., Braydich-Stolle, L. K., Schrand, A. M., Miller, J. M., Hutchison, J., Schlager, J. J. & Hussain, S. M. Surface charge of gold nanoparticles mediates mechanism of toxicity. *Nanoscale* **3**, 410–420 (2011).
21. Asati, A., Santra, S., Kaittanis, C. & Perez, J. M. Surface-charge-dependent cell localization and cytotoxicity of cerium oxide nanoparticles. *ACS Nano* **4**, 5321–5331 (2010).
22. Bhattacharjee, S., de Haan, L. H. J., Evers, N. M., Jiang, X., Marcelis, A. T. M., Zuilhof, H., Rietjens, I. M. C. M. & Alink, G. M. Role of surface charge and oxidative stress in cytotoxicity of organic monolayer-coated silicon nanoparticles towards macrophage NR8383 cells. *Particle Fibre Toxicol.* **7**, 25 (2010).
23. Thevenot, P., Cho, J., Wavhal, D., Timmons, R. B. & Tang, L. Surface chemistry influences cancer killing effect of TiO_2 nanoparticles. *Nanomed.* **4**, 226–236 (2008).
24. Maiorano, G., Sabella, S., Sorce, B., Brunetti, V., Malvindi, M. A., Cingolani, R. & Pompa, P. P. Effects of cell culture media on the dynamic formation of protein–nanoparticle bio-conjugates and influence on the cellular response. *ACS Nano* **4**, 7481–7491 (2010).
25. Hu, W., Peng, C., Lv, M., Li, X., Zhang, Y., Chen, N., Fan, C. & Huang, Q. Protein corona-mediated mitigation of cytotoxicity of graphene oxide. *ACS Nano* **5**, 3693–3700 (2011).
26. Casals, E., Pfaller, T., Duschl, A., Oostingh, G. J. & Puntes, V. Time evolution of the nanoparticle protein corona. *ACS Nano* **4**, 3623–3632 (2010).
27. Walczyk, D., Bombelli, F. B., Monopoli, M. P., Lynch, I. & Dawson, K. A. What the cell "sees" in bionanoscience, *J. Am. Chem. Soc.* **132**, 5761–5768 (2010).

Acknowledgements

This work was partially supported by the National Natural Science Foundation of China (Nos. 51011130028, 50990063 and 50973095), by Zhejiang Provincial Natural Science Foundation of China (Youth Talent Program: R4110030), Science and Technology Department of Zhejiang Provincial (Qianjiang Talent Program: 2011R10077), the Fundamental Research Funds for the Central Universities of China (No.: 2011QNA4030), and by the Interdisciplinary Laboratory for Nanoscale Science and Technology & Material Analysis Station, National Institute for Materials Science (NIMS), Japan. We thank Y. Nemoto and H. Gao for assistance with TEM measurements.

Author contributions

M.S.X. originated the work and designed the experiments. M.S.X. performed the experiments, analyzed the data and prepared the manuscript. J.L. and N.H. performed zeta potential experiments. H.I. performed XPS measurement and data analysis. Q.S.M. carried out XRD measurement and data analysis. All discussed the results.

Additional information

Supplementary information accompanies this paper at http://www.nature.com/scientificreports

Competing financial interests: The authors declare no competing financial interests.

How to cite this article: Xu, M. *et al.* Formation of Nano-Bio-Complex as Nanomaterials Dispersed in a Biological Solution for Understanding Nanobiological Interactions. *Sci. Rep.* **2**, 406; DOI:10.1038/srep00406 (2012).

Xu *et al. Journal of Nanobiotechnology* 2012, **10**:16
http://www.jnanobiotechnology.com/content/10/1/16

JOURNAL OF NANOBIOTECHNOLOGY

RESEARCH Open Access

Genotoxicity and molecular response of silver nanoparticle (NP)-based hydrogel

Liming Xu[1,2*], Xuefei Li[2], Taro Takemura[3], Nobutaka Hanagata[3], Gang Wu[2] and Laisheng Lee Chou[4*]

Abstract

Background: Since silver-nanoparticles (NPs) possess an antibacterial activity, they were commonly used in medical products and devices, food storage materials, cosmetics, various health care products, and industrial products. Various silver-NP based medical devices are available for clinical uses, such as silver-NP based dressing and silver-NP based hydrogel (silver-NP-hydrogel) for medical applications. Although the previous data have suggested silver-NPs induced toxicity in vivo and in vitro, there is lack information about the mechanisms of biological response and potential toxicity of silver-NP-hydrogel.

Methods: In this study, the genotoxicity of silver-NP-hydrogel was assayed using cytokinesis-block micronucleus (CBMN). The molecular response was studied using DNA microarray and GO pathway analysis.

Results and discussion: The results of global gene expression analysis in HeLa cells showed that thousands of genes were up- or down-regulated at 48 h of silver-NP-hydrogel exposure. Further GO pathway analysis suggested that fourteen theoretical activating signaling pathways were attributed to up-regulated genes; and three signal pathways were attributed to down-regulated genes. It was discussed that the cells protect themselves against silver NP-mediated toxicity through up-regulating metallothionein genes and anti-oxidative stress genes. The changes in DNA damage, apoptosis and mitosis pathway were closely related to silver-NP-induced cytotoxicity and chromosome damage. The down-regulation of CDC14A via mitosis pathway might play a role in potential genotoxicity induced by silver-NPs.

Conclusions: The silver-NP-hydrogel induced micronuclei formation in cellular level and broad spectrum molecular responses in gene expression level. The results of signal pathway analysis suggested that the balances between anti-ROS response and DNA damage, chromosome instability, mitosis inhibition might play important roles in silver-NP induced toxicity. The inflammatory factors were likely involved in silver-NP-hydrogel complex-induced toxic effects via JAK-STAT signal transduction pathway and immune response pathway. These biological responses eventually decide the future of the cells, survival or apoptosis.

Keywords: Silver nanoparticle-based hydrogel (silver-NP-hydrogel), Genotoxicity, Global gene expression, DNA damage, Apoptosis and mitosis pathway, JAK-STAT signal transduction pathway

Background

Since the 2000s with the development of nanotechnology, various nanomaterials have been commercially used in a wide range of areas. Due to their antibacterial activity, silver-nanoparticles (NPs) are used commonly in medical products and devices, food storage materials, cosmetics, various health care products, and industrial products. In medical applications, silver-NPs have been used for silver-based dressings [1,2], silver-coated catheters [3,4], silver-based hydrogel [5-7]. Silver-NP-hydrogel composites are composed of silver-NP and hydrogel which are used as carrier for silver particles. Most studies focused on manufacturing methods and antibacterial activity of silver-NP-hydrogel composites [5-7].

In recent years, increasing data demonstrated that silver-NPs could induce toxicity in vivo under a variety of exposure conditions including inhalation [8-10], orally [11,12] and via hypodermic injection [13]. Some in vitro studies revealed that silver-NPs could cause strong cytotoxicity in a broad spectrum of cells [14-25], such as germline stem cells

* Correspondence: xuliming@nifdc.org.cn; Lchou@bu.edu
[1]Institute for Medical Devices Control, National Institutes for Food and Drug Control (NIFDC), No. 2 Temple of Heaven, Beijing 100050, China
[4]Goldman School of Dental Medicine, Boston University, 801 Albany Street, Suite 200, Boston, MA 02118-2392, USA
Full list of author information is available at the end of the article

[15], messenchymal stem cells (hMSCs) [16-18], BRL 3A rat liver cells [19], NIH3T3 cells [20], HepG2 human hepatoma cells [21], normal human lung fibroblasts (IMR-90), human glioblastoma cells (U251) [22,23], human normal bronchial epithelial (BEAS-2B) cells [24] and HeLa cells [25]. Many studies also reported that silver-NPs induced potential genotoxicity in several types of cells [21-24,26]. With the concerns about the safety and clinical risks associated with silver-NP-based medical products, however, a little is know about the molecular mechanism of silver-NP induced toxicity.

Metal ions including silver act as catalysts and can produce reactive oxygen species (ROS) in the presence of oxygen, which is considered to be a mechanism of toxicity and genotoxicity for metal nanomaterials. Acting as signal molecules, ROS, can promote cell cycle progression and induce oxidative DNA damage [19,27-29]. CBMN assay [30] is sensitive to ROS-mediated DNA damage, making it suitable for assessing the genotoxicity potentially induced by nanomaterials. Therefore, CBMN assay was selected to assess genotoxicity of silver-NP-hydrogel in this study.

Technique of microarray provides a way of studying biocompatibility of biomaterials at molecular level [31]. The global gene expression analysis using the microarray technique could gain profiling information of nanomaterial-cell interactions [25,32,33].

In this study, in vitro genotoxicity and molecular responses of silver-NP-hydrogel were assessed by CBMN assay and global gene expression analysis. The results provided scientific evidence for understanding the biosafety and potential clinical risk of silver-NP-based products.

Results

Genotoxicity

To know whether silver-NP-hydrogel has potential genetoxicity, a CBMN assay was conducted for assessing chromosome damage by silver-NP-hydrogel in HeLa cell cultures. The results were presented as the frequency of micronucleation per 1000 BNCs (Table 1). The MMC treatment (positive control) showed a MNF of 20.6% ± 2.47, showing a significant difference compared to the NaCl solution treatment (negative control), which had a MNF of 2.5% ± 0.79 ($P < 0.05$). It confirmed that the test system worked well. There was a significant increase in the MN frequency at 20 mg/ml ($P < 0.05$), 40 mg/ml ($P < 0.05$) and 60 mg/ml ($P < 0.05$) of silver-NP-hydrogel exposure, this was not observed at the hydrogel treatment alone ($P = 0.116$). These results suggested that the silver-NP-hydrogel induced chromosome damage in HeLa cells.

Table 1 The CBMN assay of HeLa cells post-exposed to silver-NP-hydrogel and hydrogel for 24 h

Test	Dose	FMN (%)	95% Confidence Interval for mean	
			Lower Bound	Upper Bound
NC (NaCl sol.)	50 μl	2.5 ± 0.79	5.3	44.7
Hydrogel	60 mg/ml	3.7 ± 0.66	20.7	53.3
Silver-NP Gel	20 mg/ml	7.0 ± 0.82*	49.7	90.3
	40 mg/ml	8.67 ± 0.32*	78.7	94.7
	60 mg/ml	9.47 ± 0.3*	87.6	102.5
PC (MMC)	0.05 μg/ml	20.6 ± 24.7*		

Mitomycin C (MMC) was used as a positive control (PC). NaCl solution (NaCl sol.) was used as a negative control (NC). The results were presented as percentage of micronucleation frequency (FMN %) in 1000 binucleation cells. The significance of positive control compared to negative control was identified using T-Test. The significance of all test samples compared to negative control was identified using ANOVA and Dunnett tests (2-sided).
*$P < 0.05$. The data indicate the mean ± SD (n = 3).

Cellular response at molecular levels

To assess the cellular response induced by silver-NP-hydrogel exposure at the molecular level and the mechanisms of toxic effects, global gene expression and GO pathway analysis was performed using the DNA microarray technique. The graphical abstract of working process for global gene expression analysis was shown in Figure 1.

The morphological changes of cells

After exposing cells to 40 mg/ml silver-NP-hydrogel (contained 15.2 μg of silver-NPs) for 24 h and 48 h, the cells lost their normal epithelial cell morphology, becoming longer, and swelled. In contrast, cells exposed to hydrogel (without silver-NPs) did not show significant difference compared to the non-treatment control (Figure 2).

Gene expression profiling

According to the defined filtering criteria as described in "Materials and methods", the differentially expressed genes in both silver-NP-hydrogel and hydrogel alone groups, including up-regulated and down-regulated genes, are shown in Additional files 1, 2, 3, 4, 5, 6, 7 and 8. A total of 1,258 genes (Additional file 1) were up-regulated and 788 genes (Additional file 2) were down-regulated at 24 h exposure to silver-NP-hydrogel. Also, 1,532 genes (Additional file 5) were up-regulated and 824 genes (Additional file 6) were down-regulated at 24 h exposure to hydrogel alone. After the 48 h exposure, a total of 843 genes (Additional file 3) were up-regulated and 642 genes (Additional file 4) were down-regulated from silver-NP-hydrogel exposure. In contrast, 99 genes (Additional file 7) were up-regulated and 370 genes (Additional file 8) were down-regulated from exposure to hydrogel alone.

By comparing 24 h and 48 h gene expression profiling, it was observed that the 21.7% of genes that were up-regulated at 24 h post-exposure to silver-NP-hydrogel were continuously highly expressed until the 48 h exposure (273 genes, Additional file 9) (Figure 3A). This suggested that the silver-NP-hydrogel continuously induced gene up-regulation at 48 h exposure. In addition, 19.16% of the genes that were down-regulated at 24 h post-exposure, were

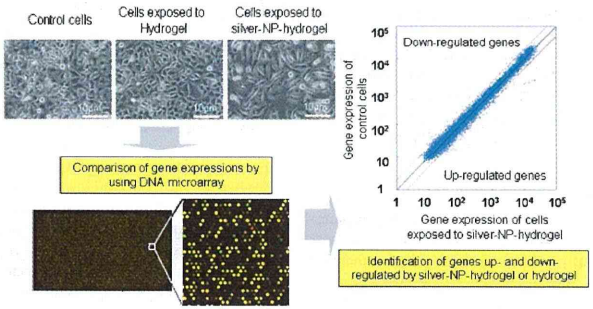

Figure 1 The graphical abstract of working process for global gene expression analysis. After exposure to silver-NP-hydrogel and Hydrogel, the treated cells and non-treatment control cells were harvested. Gene expression profiling was analysis by DNA microarray technique. The differential expressed genes were identified by comparing the gene expression levels in treated cells with that in the control cells without treatment.

continuously lower-expressed until the 48 h exposure (151 genes, Additional file 10) (Figure 3A). This suggested that the silver-NP-hydrogel continuously caused gene down-regulation at the 48 h exposure period.

In contrast, most of the up-regulated genes at 24 h exposure to hydrogel alone had recovered after continuous exposure up to 48 h. Only 1.76% of up-regulated genes at 24 h exposure continuously showed higher-expression at 48 h (27 genes, Additional file 11) (Figure 3B). This observation suggested that the gene up-regulation was a transient response in the cells against the extracellular stimulation from the hydrogel. However, 16.75% of genes that were down-regulated at 24 h post-exposure to hydrogel alone, were continuously lower-expressed until 48 h exposure (138 genes, Additional file 12) (Figure 3B). These results suggested that down-regulated genes rather than up-regulated genes might play a role in the cell response against hydrogel alone.

By further comparing changed genes common to both silver-NP-hydrogel and hydrogel alone exposure, it was found that, of the 843 up-regulated genes at 48 h silver-NP-hydrogel exposure, only 3.91% of genes were common to those expressed at hydrogel alone exposure (33 genes, Additional file 13); and 96.09% of the genes were unique for silver-NP-hydrogel exposure (Figure 3C). For the 642 down-regulated genes at 48 h of silver-NP-

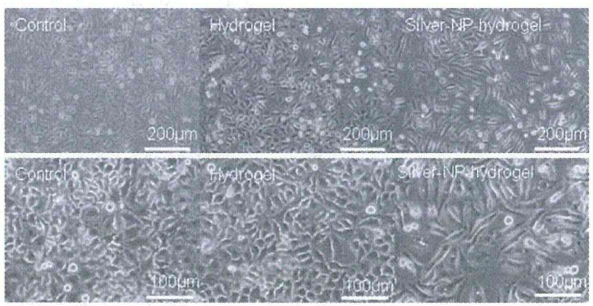

Figure 2 Cell morphological changes. The cells were post-exposed with silver-NP-hydrogel (40 mg/ml) and Hydrogel (40 mg/ml) as the study groups and with no treatment as a control for 24 h (up-panel, X 200) and 48 h (bottom-panel, X 400). The changes of cell morphology were visualized by light microscopy.

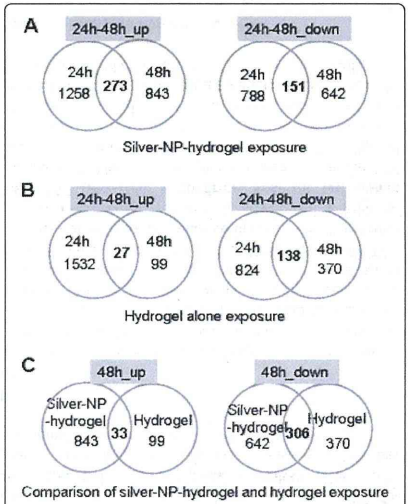

Figure 3 Gene expression profiling based on DNA microarray data. A, Up- and down-regulated genes in silver-NP-hydrogel exposed HeLa cells (Additional file 1, 2, 3 and 4); B, Up- and down-regulated genes in hydrogel alone exposed HeLa cells (Additional file 5, 6, 7 and 8); C, A comparison of common expressed genes in the silver-NP-hydrogel and hydrogel alone exposed cells (Additional file 13 and Additional file 14).

hydrogel exposure, 46.66% (306 genes, Additional file 14) of genes were common to those expressed at hydrogel alone exposure; and 53.34% of the genes were unique changes for silver-NP-hydrogel exposure (Figure 3C). These results suggested that the up-regulated genes induced by silver-NP-hydrogel could be mainly attributed to silver-NPs and that the down-regulated genes induced by silver-NP-hydrogel could be attributed in part to silver-NP and hydrogel components. It was indicated that silver-NPs could play a key role in the silver-NP-hydrogel induced toxicity, while hydrogel components might also play a role in the toxic response to silver-NP-hydrogel by down-regulating some gene expressions.

GO function analysis of differential expressed genes

Based on gene ontology (GO) biological processes, the genes which were up- and down-regulated at 48 h of silver-NP-hydrogel exposure were further analyzed using the program of GO Surfer. With the gene number-based signal pathway activation analysis, the GO pathway which has theoretically significant activation ($p < 1.0E-03$) was further picked-up as shown in Table 2 and Table 3.

Pathway analysis of GO/Biological processes showed that fourteen functional signal pathways were related to up-regulated genes at 48 h of silver-NP-hydrogel exposure (Table 2), suggesting that the up-regulated genes might play an important role in adverse cell responses. These fourteen functional signal pathways were unique for silver-NP-hydrogel exposed cells, but not common to hydrogel alone exposed cells, suggesting that the changes in functional signal pathways were attributed to silver-NPs. Under the same analysis method, in contrast, non-signal pathway which was theoretical significant activation was observed in up-regulated genes at 48 h of hydrogel alone exposure (data not shown). In addition, the most up-regulated genes at 24 h exposure had recovered at 48 h of hydrogel exposure (Figure 3B). It was further suggested that the up-regulated genes induced by the hydrogel components might not affect cell function. Several pathways were related to down-regulated genes at 48 h of silver-NP-hydrogel exposure (Table 3). These included the nucleobase, nucleoside, nucleotide and nucleic acid metabolic processes pathway, cell cycle pathway and mitosis pathway. These results suggested that the down-regulated genes might cause cell damage by affecting cell proliferation, cell cycles and mitosis. The later two pathways, being unique to silver-NP-hydrogel exposure, were not common to hydrogel alone exposure, suggesting that the changes of these functional signal pathways are mainly

Table 2 GO function analysis of differential expressed genes at 48 h exposure of silver-NP-hydrogel

Functional GO pathway	REF.-LIST*/Up-exp#/expected$	P value
cell communication	4365/231/174.28	p = 1.04E-06
cell-cell signaling	1331/81/53.14	p = 2.14E-04
cell adhesion	1333/77/53.22	p = 8.67E-04
signal transduction	4191/215/167.34	p = 2.37E-05
intracellular signaling cascade (JAK-STAT cascade)	1568/102/62.61	p = 1.02E-06
metabolic process	8267/373/330.08	p = 7.32E-04
lipid metabolic process	1119/94/44.68	p = 7.32E-12
carbohydrate metabolic process	952/69/38.01	p = 1.08E-06
response to stimulus	1798/119/71.79	p = 7.96E-08
transport	2857/164/114.07	p = 6.18E-07
endocytosis	575/43/22.96	p = 9.23E-05
cellular defense response	457/38/18.25	p = 2.75E-05
immune system process	2628/171/104.93	p = 7.69E-11
immune response	756/52/30.19	p = 1.41E-04

* reference list, that is all genes number related to the GO pathway;
# up-expressed genes number in this study;
$ expected minimum genes number for activating of signal pathway.
Based on the gene ontology (GO) biological process, the GO pathway, which has theoretically significant activation ($p < 1.0E-03$), related to up-regulated genes.

Table 3 GO function analysis of differential expressed genes at 48 h exposure of silver-NP-hydrogel

Functional GO pathway	REF.-LIST*/Down-exp#/expected$	P value
nucleobase, nucleoside, nucleotide and nucleic acid metabolic processes	3825/138/81.84	p = 8.40E-12
cell cycle	1840/62/39.37	p = 2.60E-04
mitosis	635/27/13.59	p = 6.90E-04

* reference list, that is all genes number related to the GO pathway;
# down-expressed genes number in this study;
$ expected minimum genes number for activating of signal pathway.
Based on the gene ontology (GO) biological process, the GO pathway, which has theoretically significant activation ($p < 1.0E-03$), related to down-regulated genes.

attributed to silver-NPs. These events were considered to be closely involved with cytotoxicity and genotoxicity. At 48 h of hydrogel exposure, three pathways related to down-regulated genes were also showed theoretical significant activation. They included a metabolic process ($p = 4.02E-04$), nucleobase, nucleoside, nucleotide and nucleic acid metabolic processes ($p = 1.69E-10$) and the primary metabolic process ($p = 2.97E-04$). These results suggested that the down-regulated genes induced by hydrogel alone might have some effect on cell proliferation and metabolism.

Real-time PCR verification of differential expressed genes

To verify the reliability of differential expressed gene identified by the DNA microarray, five genes selected from up- and down-regulated genes expressed in silver-NP-hydrogel 48 h exposure were further examined with real-time PCR detection. The results showed that the gene expression was basically consistent with that of the microarray analysis, indicating a good reliability and reproducibility of the microarray in the current study (Table 4).

Discussion

Genotoxicity evaluation is an idea assessment of biosafety at molecular level for nanomaterials-based medical devices. In this study, a significant increases in the micronucleation frequency (MNF) of HeLa cells was induced by the silver-NP-hydrogel exposure at concentrations of 20-, 40-, and 60-mg/ml (in medium), compared to the negative control ($P < 0.05$), suggesting that the silver-NP-hydrogel has a potential risk of genotoxicity. The study also showed that hydrogel alone did not show significant change, compared to the negative control, suggesting that genotoxicity caused by silver-NP-hydrogel was attributed to silver-NPs. Kawata et al. demonstrated that exposure to 1.0 μg/ml of silver-NPs (7–10 nm in size) induced MNF up to 47.9% in the HepG2 cell line [21]. AshaRani et al. reported that exposure at the 25 μg/ml of silver-NPs (6–20 nm in size) induced chromosomal aberrations in 10% of the IMR-90 normal cell line, and in 20% of the U251 cancer cell line [22,23]. In the comet assay and micronucleus (MN) assay for BEAS-2B cells, silver-NPs (43–260 nm in size, dispersed in medium) stimulated DNA breakage and MN formation in a dose-dependent manner [24]. In this study, the size of silver nanoparticles contained in silver-NP-hydrogel ranged from 5 nm to 30 nm (observed by TEM, dispersed in water). Number of studies has reported for the in vivo genotoxicity and carcinogenicity by silver-NPs. Study by Kim et al. reported that there was no genotoxic effect in rats after 28 days oral exposure to Ag NPs [11]. Kim et al. also reported that no genotoxic effect in rats after 90 days inhalation of Ag NPs [34]. In contrast, however, our recent study reported that silver-NP-hydrogel induced micronuclei, nuclei disruption, chromatin concentration and cell apoptosis in rabbit reproductive organ tissues in silver-NP-hydrogel administration through the vagina [35]. The difference of findings in potential genotoxic and carcinogenic risks of nanomaterials is possibly due to the insufficient characterization of test material, difference in the experimental design, use of different animal models and species, difference in dosimetry, and different targeting organs [36]. It was known that confirmation of asbestos nanofiber as a carcinogen in Japan took over 10 years [37]. Since the silver nanoparticles are still widely used clinically in some countries, it is important to gain a better understanding of their genotoxicity and carcinogenecity.

Table 4 The gene expression detected by real-time PCR and detected by DNA microarray at 48 h exposure of silver-NP-hydrogel

determination	IL1A	HMOX1	DDIT3	MT1F	PDGFRB
Real-time PCR ($2^{-\nabla\nabla Ct}$)	15.97	6.58	8.18	82.96	0.4
DNA microarray (fold changes)	2.76	2.41	2.17	5.63	−2.14

Two important molecular mechanisms were considered to be involved in the in vitro toxicity and genotoxicity induced by silver-NP-hydrogel, as further discussed below.

The balance between anti-ROS-toxicity and DNA damage

From the data in this study, the signaling pathways and regulatory proteins involved in anti-ROS-toxicity, DNA damage, apoptosis, cell cycles and mitosis might be associated with genotoxicity caused by silver-NP-hydrogel.

Metallothioneins (MTs) are considered to be essential biomarkers in metal-induced toxicity [38] as facilitating metal detoxification and protection from free radicals [39]. A report on heavy metal toxicity in Javanese medaka showed that MT upregulation occurs in silver mediated toxicity [40]. Hemeoxygenase-1 (HO-1) is an ROS sensor and a cryoprotective agent possessing antioxidant and anti-inflammatory properties. HO-1 breaks down heme to antioxidant biliverdin, carbon monoxide and iron under stress conditions [41,42]. It was reported that oxidative stress response genes (superoxide dismutase 2, glutathione reductase 1, etc.) in mouse brain following silver-NP exposure were upregulated [43]. In the present study, 10 metal-

lothionein genes (MT1F, MT1A, MT2A, MT1B, MT1G, MT1H, MT1X, MT1L, MT1M, MT1E), HO-1 and oxidative stress induced growth inhibitor 1 (OSGIN1) were significantly up-regulated at 48 h of silver-NP-hydrogel exposure [Additional file 5 and Additional file 6]. All these molecules are believed to protect cells against metal-induced ROS toxicity. Metal ions including silver act as catalysts and can produce reactive oxygen species in the presence of oxygen, which is thought to be a mechanism of toxicity. Previous studies showed that silver-NPs increase the production of intracellular ROS [20]. The ROS can act as signal molecules promoting cell cycle progression, and can induce oxidative DNA damage [27-29]. We previously reported that HeLa cells exposed to silver-NPs consistently over-express isoforms of metallothionein (MT1A, MT1F, MT1G, MT1X, and MT2A) [25]. AshaRani et al. reported that the MT-1 F and HO-1 were upregulated in IMR-90 cells following silver-NP treatment [22]. Kawata et al. also reported that three metallothionein genes (MT1H, MT1X, MT2A) were significantly upregulated in HepG2 cells exposed to silver-NPs [21]. These studies suggested that the cells protect themselves against silver NP-mediated toxicity through up-regulating metallothionein genes and oxidative stress induced genes.

On the other hand, the genes which are related to the DNA damage and apoptosis, such as DNA-damage-inducible transcript 3 (DDIT3), caspase 1, and apoptosis-related cysteine peptidase (CASP1) were up-regulated by silver NPs. Changes in chromosome related genes (24 genes up-regulated and 26 genes down-regulated) (Additional file 3 and Additional file 4) found in this study might damage the chromosomes. Apoptosis inhibitors, such as BCL2 interacting protein (HRK), BIK (BCL2-interacting killer, apoptosis-inducing), Fas apoptotic inhibitory, molecule 3 (FAIM3), apoptosis inhibitor (FKSG2), suppression of tumorigenicity 13 (ST13), growth arrest and DNA-damage-inducible, alpha (GADD45A) were also significantly up-regulated. This suggested that silver nanoparticles induced apoptosis via a mitochondrial pathway. Apoptosis and chromosome damage could be subsequently involved in cytotoxicity and genotoxicity.

In addition, analysis of the activating signal pathways in this study also suggested that cell cycles and the mitosis signal pathway were significantly down-regulated, which was uniquely represented at the silver-NP-hydrogel 48 h exposure. These pathways are considered to be closely involved in cell proliferation, apoptosis and tumorigenesis progression. There were 62 genes related to cell cycle signal pathways. Among them, 27 genes were related to mitosis pathway (Additional file 15). In these genes, cell division cycle 14 homolog A (CDC14A) showed a 13 -fold ($\log_2 = -3.71$) down-regulation. CDC14A is a member of the dual specificity protein tyrosine phosphatase family. It is highly similar to saccharomyces cerevisiae Cdc14, a protein tyrosine phosphatase involved in the exit of cell mitosis and initiation of DNA replication, playing a role in cell cycle control. CDC14A protein has been shown to interact with and dephosphorylate the tumor suppressor protein p53, and is thought to regulate the function of p53 [44]. Human CDC14A shares sequence similarity with the recently identified tumor suppressor, MMAC1/PTEN/TEP1. CDC14A is located at chromosome band 1p21, a region that has been shown to exhibit loss of heterozygosity in highly differentiated breast carcinoma and malignant mesothelioma. Thus, CDC14A has been thought to be a tumor suppressor gene [44]. The down-regulation of CDC14A in this study suggested that it might play a role in the potential genotoxicity induced by silver-NP-hydrogel.

As summarized in Figure 4, the balance between anti-ROS-toxicity and DNA damage, apoptosis, mitosis inhibition of the cells could be the main events which decide the future of the cells.

JAK-STAT signal transduction pathway

The JAK-STAT (Janus kinase/signal transducers and activators of transcription) cascade is an important signal pathway which affects basic cell functions such as cell growth, differentiation and apoptosis [45]. STAT is a signal transducer and activator of transcription. It conveys or transduces the signal from the receptor-JAK (Janus Kinase) complex to the DNA in the cell nucleus [45]. In mammals, the JAK-STAT signal pathway is the principal signaling mechanism for a wide array of cytokines and growth factors [45,46]. Defects in JAK-STAT proteins can result in immune deficiency disease and cancer [45]. JAKs, which have tyrosine kinase activity, bind to some cell surface cytokine receptors. So, the cytokines, as ligands, through binding to the receptor would trigger activation of JAKs [46-50]. In this

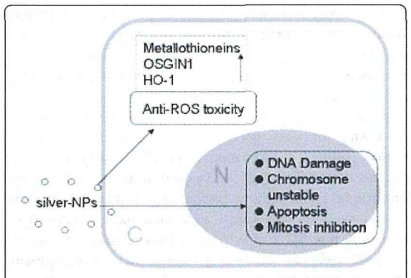

Figure 4 Scheme of molecular mechanisms of cellular response against silver-NP-hydrogel exposed. The balance among anti-ROS-toxicity and DNA damage, apoptosis, mitosis inhibition of the cells might play important role in cytotoxicity. These responses were mainly induced by silver-NPs contained in silver-NP-hydrogel.

study, it was found that silver-NP-hydrogel exposure induced JAK-STAT cascade-related gene up-regulation, not only at 24 h exposure but also for 48 h exposure [Additional file 5 and Additional file 6], and implied that the silver-NP-hydrogel might play a role in JAK-STAT pathway.

It was found by further analysis that many interferon-induced proteins (IFI), interferon-induced protein in the tetratricopeptide (IFIT) family, and interleukin (IL) family were up-regulated (Additional file 5 and Additional file 6). These inflammatory factors acting as ligands while they participate in immune response pathway, may also trigger the activation of JAK-STAT signal pathway through binding to the JAK receptor.

Conclusions

In summary, the silver-NP-hydrogel induced micronuleus formation in HeLa cells. The toxic effects caused by silver-NP-hydrogel arrived mainly from silver-NPs. Based on DNA microarray and GO pathway analysis, the molecular response and mechanisms of toxicity induced by silver-NP-hydrogel might relate to some up-regulated genes involved in fourteen theoretical activating signaling pathways and to some down-regulated genes involved in three signal pathways at 48 h of silver-NP-hydrogel exposure in HeLa cells. These signal pathways play important roles in metabolisms, cell communication, signal transduction, cellular defense response, transport, cell cycles and mitosis. The down-regulation of CDC14A via mitosis pathway suggested that it may play a role in the potential genotoxicity induced by silver-NP. The balances between anti-ROS response and DNA damage, chromosome instability and mitosis inhibition might play important roles in silver-NP induced toxicity. It was also demonstrated that activations of both JAK-STAT signal transduction pathway and immune response pathway could be involved in the mechanisms of toxicity caused by silver-NP-hydrogel.

Materials and methods

Test materials and chemicals

Silver-NP-based hydrogel (silver-NP-hydrogel) used in this study was a clinical available product, and has been used in clinic for treating cervicitis and cervical erosion of women. The product provided by Egeta Co. (Shenzhen, China, Batch Number 090701) was manufactured by simply mixing aqueous silver-NP solution (concentration of 2,000 ppm, purchased from Nanux, Korea, Cat. No. SL1105001) and hydrogel components to achieve a concentration of 0.38 μg/mg (silver- NP-hydrogel). The silver NPs were not coated by any compounds such as PVP, citrate or BSA. To determine the NP size distribution, silver-NP-hydrogel was dissolved in water. Then, the silver particles were collected by centrifuging and placed on a cuppernet for evaluation of size distribution by TEM (Additional file 16: Figure S1). As determined through TEM, the size distribution of the nanoparticles was as follows: 3–5 nm, 47.9%; 5–10 nm, 50.8%; 10–30 nm, 1.3%. The hydrogel was composed of sterile water, glycerine, carbomer and triethanolamine (TEA). The hydrogel component alone (without silver-NP) was used as the compared control.

Cytochalasin B (Cyt-B), Mitomycin C (MMC) and Dimethyl sulfoxide (DMSO) were purchased from Sigma-Aldrich (USA). The Cyt-B was dissolved in DMSO (2.0 mg/ml), and the MMC was dissolved in NaCl solution (10 μg/ml) for use as a stock solution. All solutions were sterilized by using 0.2 μm-pore film and stored at −20°C.

Cell culture and treatment

Silver-NP-hydrogel is currently a clinical product on the markets and is commonly used for treating cervicitis and cervical erosion of women. Therefore, the HeLa cell line was chosen as a cell model in this study. HeLa cells were originally purchased from RIKEN (Wako, Japan) with a RIKEN Cell line number. RCB0007. The cells were cultured in DMEM (GIBCO, USA), with 10% FBS (GIBCO, USA) and 100 U/ml penicillin/100 μg/ml streptomycin (GIBCO, USA), in a humidified 5% CO_2 atmosphere at 37°C.

To determine a suitable concentration of silver-NP-hydrogel for the study, a preliminary experiment was performed by adding silver-NP-hydrogel to culture medium at concentrations of 2.5, 5, 10, 20, 40, and 60 mg/ml. After ultrasonic treatment (300 W, 42 kHz,) for 10 min, the media with various concentrations of silver-NP-hydrogel was applied to cells which had been pre-cultured for 24 h (70–80% confluence), and the cells were then cultured for another 24 h. Cell viability was determined using a methyl tetrazolium (MTT) assay by measuring the optical density of the formazan product. Briefly, after the exposure to silver-NP-hydrogel solution, the cells were washed. A mixture of 20 μl of MTT (5 mg/ml) and 100 μl of non-phenol-red medium were added to the cells, and incubated for 4 h. After through washes and DMSO treatment, 100 μl of the supernatant of each sample was transferred for optical density (OD) detection. The assay was performed using a plate reader at a wavelength 570 nm, with 630 nm as the reference wavelength. The results represented a percentage of the relative viability of cells against to the untreated control. Based on this preliminary experiment, a middle-level viability inhibition of the cells, compared to that in the non-treatment control cells, was found at a concentration (IC50) about 40 mg/ml of silver-NP-hydrogel (in culture media) which containing 15.2 μg/ml of silver-NPs. This concentration was determined according to the concentration-relative cell viability (%) curve equation, and the non-treatment control cell viability (OD level) was served as 100%. An EC50 NP concentration was selected also because the EC50 or IC50 is a conventional coefficient in ISO and OECD standards for toxicity